UPPSALA
UNIVERSITET

ELEKTRO-MFE 25007

Degree project 30 credits

December 2025

AC Collection Grid Design for Large Scale Offshore Floating Photovoltaic Power Plants

Zeno Lucio Michelotto

UPPSALA UNIVERSITET

AC Collection Grid Design for Large Scale Offshore Floating Photovoltaic Power Plants

Zeno Lucio Michelotto

Abstract

Floating photovoltaic has emerged as a promising solution for harvesting solar energy while minimising land use. In particular, offshore floating photovoltaic (OFPV) installations present unique challenges related to the implementation in the marine environment. This project examines the offshore installation of scalable floating photovoltaic parks, focusing on the electrical requirements and power quality issues associated with connecting such solar farms to the alternating current (AC) grid via power converters.

Initially, standards and guidelines for OFPV deployment were identified through literature analysis. These guidelines have been used as a reference to determine the requirements for electrical equipment (cabling, inverters and transformers) for grid connection. A detailed OFPV park model was then implemented in PSCAD, featuring twelve clusters (each with four PV arrays, four string inverters with LCL harmonic filters, and a transformer), for a total capacity of nearly 20 MW. The model components reflect the characteristics of real devices that have been identified as appropriate for OFPV implementation through literature and market research.

A selection of power conversion devices suitable for OFPV deployment has been listed among the results, along with the findings from PSCAD simulations conducted under varying conditions to investigate harmonic content and optimise filter tuning. It was noted that properly tuned harmonic filters were necessary to obtain effective power production. Furthermore, changes in the irradiance rate influenced significantly the performance of the model and were found to be closely connected to filter tuning parameters. Additionally, cabling losses were estimated using manufacturer data to ensure transmission losses remain below 3%.

Finally, this study presents several strategies for improved harmonic mitigation and enhanced grid connection, while discussing other potential challenges encountered by the electrical equipment in such applications.

Faculty of Science and Technology

Uppsala University, Uppsala

Supervisor: Irina Temiz Subject reader: Janaina Goncalves de Oliveira

Examiner: Irina Temiz

Popular Scientific Summary

Floating solar panels (or floating photovoltaic) are an innovative technology developed to harness the energy of the sun without occupying valuable land space. In particular, placing these panels on floating platforms in the offshore/marine environment (in the sea or in the ocean) opens up new possibilities for clean energy generation, together with unique technical challenges; especially when it comes to connecting these solar farms to the standard electrical grid.

This project explores the requisites to connect offshore solar parks to the grid. First, existing standards and guidelines were reviewed to determine the required characteristics of electrical equipment (such as cables, inverters, and transformers) necessary for a reliable connection. Next, a detailed model of an offshore solar park was built and analysed using specialized simulation software (PSCAD). This model was used to study how the system behaves under varying conditions.

A central focus was to ensure the quality of the electricity produced in terms of total harmonic distortion: in any power system, unwanted electrical disturbances (known as harmonics) can reduce efficiency. The software simulations helped determine the optimal parameters to tune the filters dedicated to minimize these disturbances.

It was observed that changes in the sun irradiance strongly affect the performance and power quality of such solar parks, requiring further filter tuning. Also, cable length and cable losses were estimated to ensure proper energy transmission.

In short, this study outlines the key requirements and key challenges involved with connecting offshore floating solar parks to the electrical grid, to offer insights for future efforts to implement and scale up large floating photovoltaic installations.

Contents

List of abbreviations

Abbreviation	Definition
AC	Alternating Current
DC	Direct Current
EMC	Electromagnetic Compatibility
FFT	Fast Fourier Transform
FPV	Floating Photovoltaic
GFMI	Grid Forming Inverter
IP	Ingress Protection
MPP	Maximum Power Point
MPPT	Maximum Power Point Tracking
OFPV	Offshore Floating Photovoltaic
PCC	Point of Common Coupling
PERC	Passivated Emitter and Rear Cell
PLL	Phase-Locked Loop
PV	Photovoltaic
SCR	Short-circuit Ratio
STC	Standard Test Conditions
THD	Total Harmonic Distortion
VSI	Voltage Source Inverter

1. Introduction

1.1 Project Motivation

In the context of the current climate crisis, increase of the world population and therefore steady growth of global energy consumption, more and more attention is being diverted to the deployment and full transition to renewable energies. Hence, it comes as no surprise that the last few years have seen a massive increase in global renewable capacity, with the photovoltaic (PV) sector seeing the fastest growth rate [1]. As solar farms increase in size and power capacity year by year, the first floating photovoltaic (FPV) plants are being deployed offshore and on bodies of water such as lakes and water reservoirs, to further exploit the solar power potential without the burden of occupying land that could be used for other purposes (agriculture, residential, etc…). FPV systems present a wide range of advantages and opportunities, but also a whole set of challenges related to the deployment on water: especially considering the installation on marine environment, where floating solar farms face weight and size limitations, motion and oscillations (potentially particularly damaging for the power electronics included in the system), salty and humid environment, and more.

Considering the issues and challenges mentioned, this project focuses on the offshore deployment of large floating photovoltaic plants, in line with the EU-SCORES research project [2] funded by the European Union/European Commission through the Horizon 2020 funding programme to investigate and demonstrate the efficacy of offshore scalable multi-source renewable energy parks. In particular, the objective of this project is to examine the requirements for connecting such floating solar parks to the Alternating Current (AC) transmission grid, with particular focus on the specifics of the power converters (inverters and transformers) to be deployed for such purposes. Furthermore, this study aims to investigate possible issues related with the power parks considered, with particular attention to the harmonic content caused by using power electronics with switching components and possible mitigating solutions. Thus, this project ultimately aims to serve as a pilot study for future work considering the best practices for implementing AC connection of offshore floating photovoltaic (OFPV) parks.

Hence, for the mentioned purposes the system analysed through this project is composed of photovoltaic modules arranged in PV arrays, power inverters, harmonic filters, power transformers, the AC transmission grid, and the cabling connecting all the different components. This system serves as a model for the hypothetical implementation of an OFPV farm within a multi-source renewable energy park located off the Dutch coast in the North Sea, in line with the EU-SCORES objectives [2].

1.2 Aims, objectives, and limitations

This project aims to investigate the electrical requirements for AC connection of offshore FPV farms, focusing on power conversion devices such as inverters and transformers and possible power quality issues related to their usage. Such devices convert the Direct Current (DC) harvested from the solar panels into high voltage AC current suitable to be injected into the transmission grid, and they are widely used in “standard” land-based PV farms. However, because of floating offshore systems being still a relatively new technology, the impact of marine weather conditions on the functioning and efficiency of power electronics still has not been analysed thoroughly.

Hence, the objective of this project has been to determine the necessary characteristics and investigate for suitable inverter and transformer models to be utilised for such large scale offshore FPV farms, as well as to analyse the harmonic content and power quality issues of such systems by using a software model simulating the operation of an FPV farm (including PV arrays, inverters, transformers, and connection to the AC grid) under different irradiance and grid strength conditions. The components modeled in the software simulation (such as the PV panels, inverters, and transformers) were designed according to the characteristics found in the datasheets of models deemed suitable for offshore deployment, to better simulate an actual OFPV park.

Specific objectives:

- Identify the characteristics and requirements for the electrical equipment (and specifically inverters and transformers) to be deployed in offshore solar parks;
- Select a sample of models of inverters and transformers suitable for OFPV deployment;
- Implement a software model simulating an OFPV park, including PV arrays, inverters, transformers, and connection to the AC grid;
- Evaluate the harmonic content and power quality of the implemented model under different conditions in terms of irradiance rate and grid strength.

There have been a few limitations potentially compromising the completeness and accuracy of this work, namely:

- Time constraints, as this project has been part of a master's thesis course;
- Limited availability of open access information on power conversion models and their technical characteristics, especially regarding electrical transformers;
- Lack of prior research studies on the topic, as offshore FPV is a relatively new technology and there have been very little scientific publications to utilise as guidance/comparison at the time of execution of this project.

2. Theory background

2.1 Floating photovoltaic systems

The first commercialised floating photovoltaic system was installed by SPG Solar in July 2007 in a freshwater reservoir within a winery in California, consisting of around 400 kW power capacity (including both floating and land-based PV arrays); it was followed shortly thereafter by a 20 kW FPV plant deployed (also in 2007) in the Aichi prefecture in Japan by the National Institute of Advanced Industrial Science and Technology. From then on, FPV systems have been tested and adopted in several other countries all over the world, with China emerging as the world’s largest market for floating solar plants. In 2021, an OFPV system of 3 MW power capacity was implemented in Belgium as a complementary power plant coupled to an offshore wind farm [3, 4].

Currently, most FPV plants have been deployed in freshwater bodies (such as lakes, ponds, and hydropower reservoirs) as those environments do not present the same set of challenges related to marine environments, for instance the presence of strong winds, wave motion, and water salinity. However, marine implementations of floating solar parks have gained industry interest in the last years, with China and the Netherlands being the first countries to deploy this technology offshore [3].

Commonly, a floating PV system consists of the following components: the PV panels, the floaters, the anchoring and mooring system, the electrical cabling, and eventually an inverter (Fig. 1 and Fig. 2).

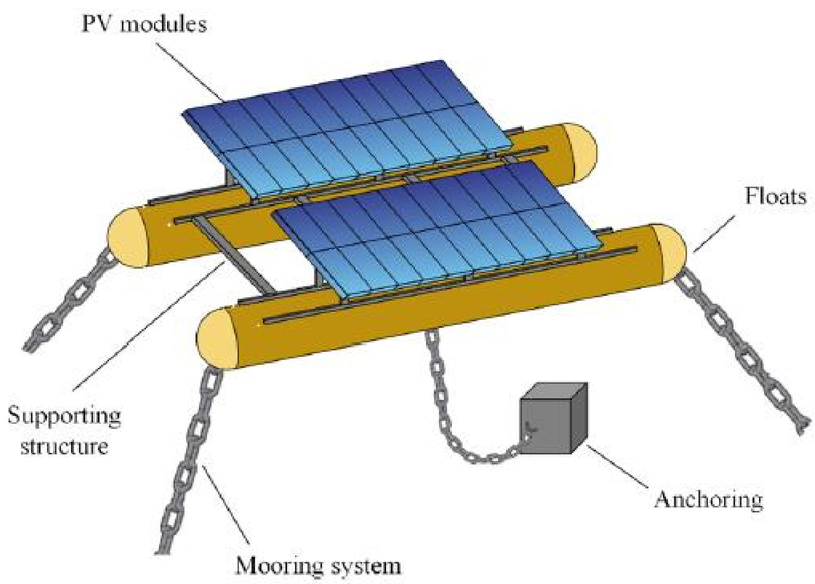

Fig. 1: Structural components of a FPV system [5].

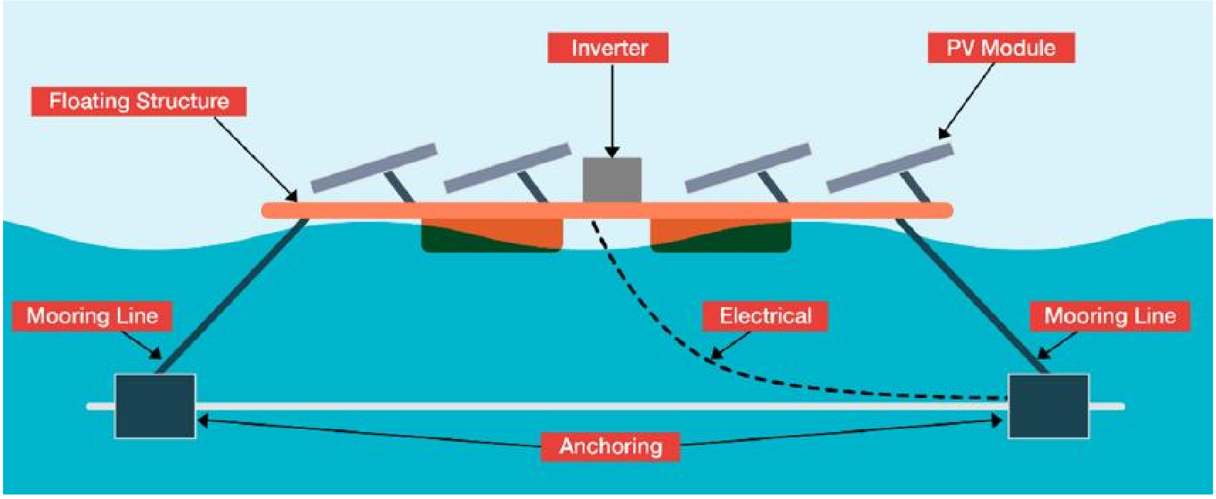

Fig. 2: Main components of a FPV system [3].

Over the years several studies have been conducted to examine the possibilities related to deploying OFPV plants around the world. Trapani et al. [6] studied the advantages related to the offshore deployment of PV systems in Europe and proposed a model utilising thin-film PV modules in 2013. Lee et al. [7] in 2015 proposed an improved model of an offshore PV park, analysing the effect on photovoltaic electricity production of parameters such as the angle between the PV panels and the irradiance. Liu et al. [8] in 2017 executed a comparison between conventional (land-based) solar plants and floating photovoltaic plants, determining that there are several advantages related to the FPV implementation, including savings in terms of land usage and water resources, as well as enhanced PV electricity production. Golroodbari et al. [9] also compared land-based and floating solar parks in 2020, including a sea waves model in their study to determine the irradiation on the tilted floating PV modules; they also determined the annual electricity production from the OFPV plant to be around 13% higher than the conventional PV park. In 2020 Kim et al. [10] designed and examined the performance of a 500 kW capacity FPV system characterised by structural components composed of high-durability steel, resulting in increased resistance to corrosion and enhanced durability.

With the increasing progress in the research on offshore floating photovoltaic solutions, several commercial projects have been deployed or are on the way to be deployed. Some notable examples include: the Taiwanese company Chenya Energy completed a 181 MWp offshore park off the coast of Taiwan in 2021, with future plans to further expand its capacity [11]; in Singapore, the solar energy developer Sunseap Group installed a 5 MW OFPV plant [12]; two offshore solar plants installed in the Dutch North Sea by the company Oceans of Energy, including a 50 kW park located near-shore (less than 1 km from the coast) and a 17 kW farm installed in open sea (at around 15 km from the coast) [13].

From the data gathered by several studies, there are several benefits and advantages related to OFPV systems, such as reduced water evaporation (and hence savings in terms of water resources), the reduced use of land resources, and the increased efficiency of solar modules thanks to the cooling effect of the water body and the water evaporating. Some challenges and possible issues have also been identified. These include the difficulties related to installation in an offshore or open sea environment (clearances for FPV projects, waterbody ownership, transportation of heavy structures), as well as the challenges linked to corrosion and accelerated degradation because of contact with sea water, potentially compromising the durability of such systems. Offshore floating solar farms being subjected to erratic or sudden movement due to strong winds and waves also could result in heavy loads on the structural components, potentially shortening the lifetime of these projects. Furthermore, FPV (and OFPV especially) is still a relatively new and immature sector, resulting in high installation and maintenance costs and a lack of data and technical guidelines [3, 14].

Aside from the components strictly making part of the FPV system (depicted in Fig. 1 and Fig. 2), a floating photovoltaic farm to be connected to the AC grid also includes cabling, power conversion devices and the connection to the transmission grid. Hence, the equipment needed for this kind of farms is composed of: the PV modules, the floaters/pontoons, the mooring and anchoring system, the cabling, the inverters, the transformers, and the connection to the transmission grid (a schematic including the components listed is depicted in Fig. 3). Through this project the topics related to mooring, anchoring and structural components were not considered, as the main focus was the electrical network and electrical connection of the OFPV park.

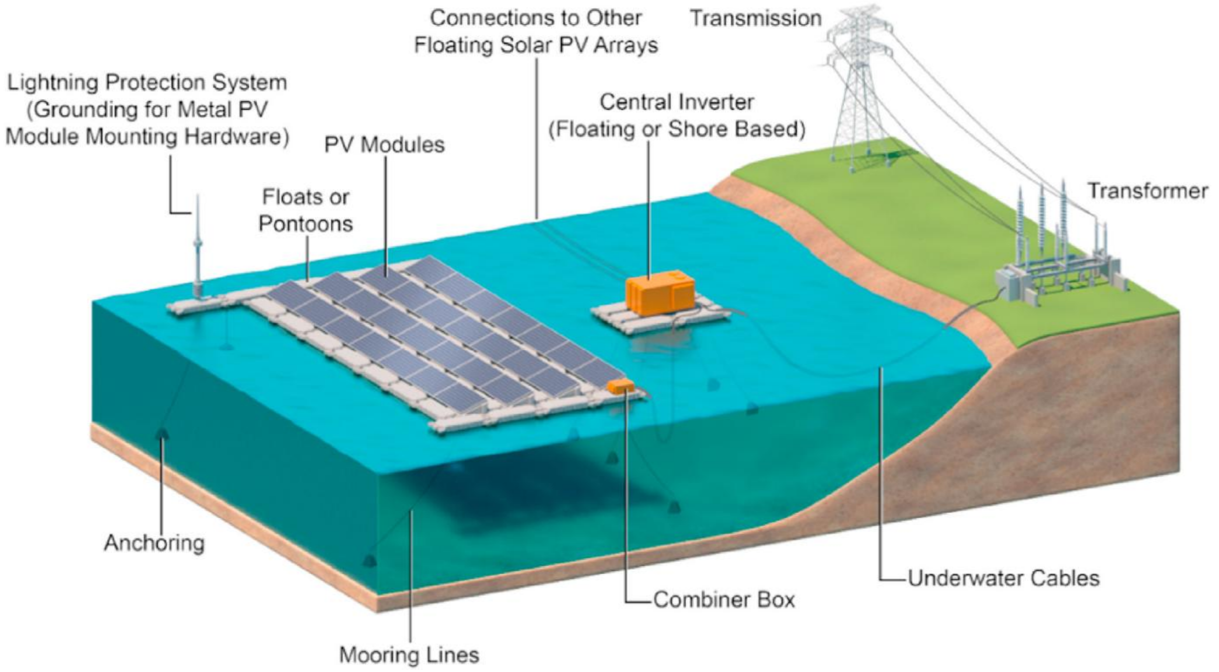

Fig. 3: Key components of an OFPV farm [15].

2.2 Photovoltaic panels

The photovoltaic technology relies on semiconductor materials (characterised by an electrical conductivity in-between that of insulators and conductors) to convert sunlight into electrical energy: as the PV material is exposed to light, the energy of the light particles (photons) is transmitted to the electrons in the solar cell, setting such particles in motion and therefore generating a flow of electrical direct current. The specific amount of electricity generated by the solar PV cell depends on the characteristics of the light colliding with the photovoltaic material, as well as on the technical specifications of the solar cell. To maximise the electrical output generated by the PV cells, they are connected and assembled in modules (or panels), which can be further connected into strings (or arrays) of PV modules, depending on the power requirements of the system at hand [16, 17].

Depending on the structure and material composing the photovoltaic cells, the PV panels can be divided into several categories. Monocrystalline silicon panels (or single-crystal panels) are composed of a pure silicon crystal cut into several sheets; this kind of PV module is the most efficient (reaching an efficiency rating of around 20%) and long-lasting due to its uniform composition. Passivated Emitter and Rear Cell (PERC) panels bring an improvement to standard monocrystalline panels by incorporating a reflective passivation layer on the back of the solar cells, which results in a reduction of the losses due to electron recombination (when electrons lose their energy before contributing to electricity generation), enhanced sunlight absorption and overall increment in efficiency. Polycrystalline solar panels, instead, are composed of different silicon crystals that are melted and poured into a square mold; while this makes them more affordable than single-crystal modules, it also causes a lower efficiency (around 16%) as well as a lower heat tolerance, further decreasing their efficiency in high-temperature environments. Finally, thin-film solar panels are composed by stacking several layers of photovoltaic materials on a rigid glass-like substrate used as a base; unlike crystalline panels, for which only silicon is used, this type of panels can be composed of different materials, including among others: cadmium telluride (for CdTe panels), amorphous silicon (a-Si panels), copper indium gallium selenide (CIGS panels). This type of PV modules presents the lowest manufacturing costs among other types, as well as the lowest efficiency range (around 7-13%) [18, 19].

2.3 Power inverters

As per conventional land-based photovoltaic plants, for OFPV parks to be connected to an electrical grid (so that the PV-generated electricity can be transmitted and distributed to end users), some power electronics devices are usually needed. That is because the photovoltaic modules harvest DC current, meanwhile most electrical grids transmit AC current. Hence, a need for devices such as solar inverters, that convert the power generated by the PV modules to characteristics suitable for connection to the electrical grid.

Inverters at their core are circuits that transfer power from a DC source to an AC load, creating an AC output from a DC input using switches. One of the simplest examples of that is a full-bridge converter (Fig. 4) with a switching scheme producing a square wave output voltage. Concretely, most inverters used in commercial applications are three-phase output inverters, with a schematic like the one presented in Fig. 5 [20].

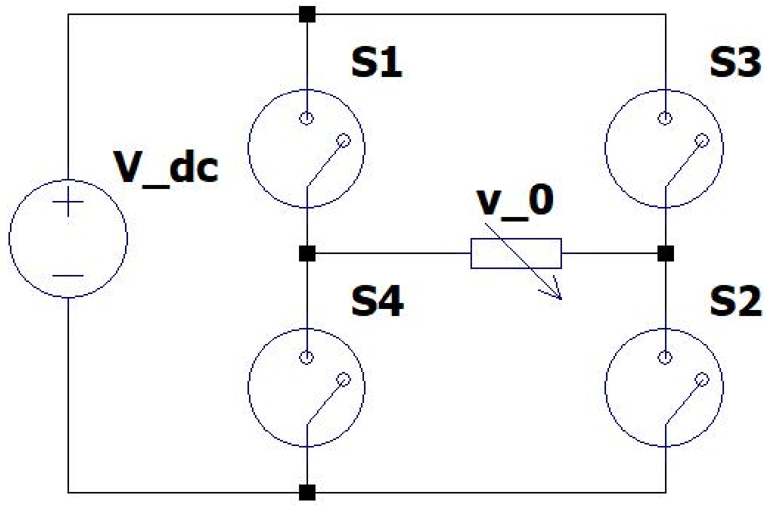

Fig. 4: Schematic of a full-bridge converter, converting DC input voltage V_{DC} to AC output v_0 by the use of the switches S_1, S_2, S_3 and S_4 (from own LTSpice circuit diagram).

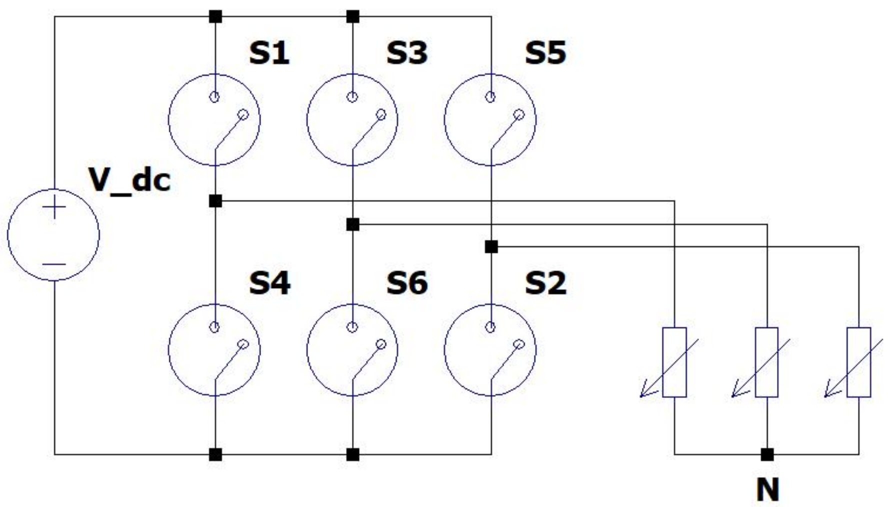

Fig. 5: Schematic of a three-phase inverter, converting DC input voltage V_{DC} to three-phase AC output by the use of six switches and transmitting it to a load N (from own LTSpice circuit diagram).

Furthermore, for inverters utilised in photovoltaic applications (solar inverters) the mode of operation is much more complex, as the power conversion is controlled by Maximum Power Point Tracking (MPPT). In short, the output power generated by the photovoltaic modules varies depending on the ambient temperature and the irradiance level. Thus, as the I-V and P-V curves change by the values assumed by the temperature and the irradiance, the maximum power point (MPP) delivering the maximum output power varies as well. Partial shading conditions (when PV systems are subjected to non-uniform solar irradiation because of for example a cloud or neighbouring object) significantly alter the shape of the power curves, making the identification of the MPP even more challenging (Fig. 6) [21, 22].

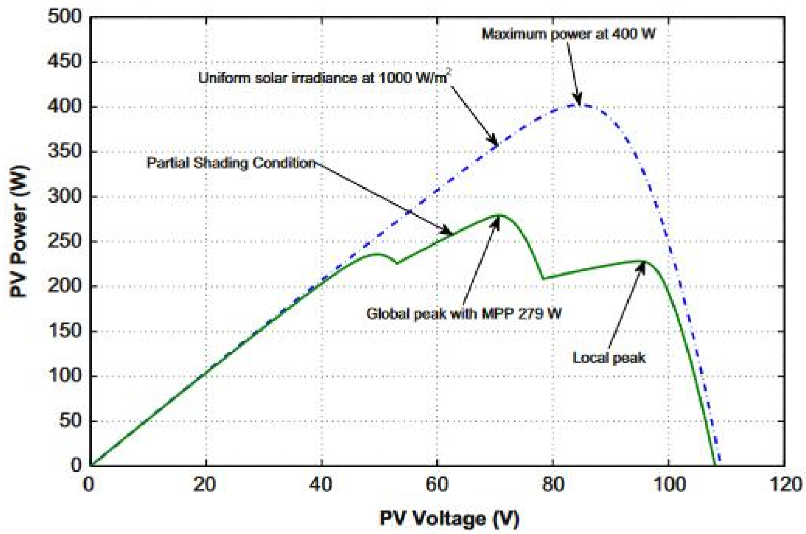

Fig. 6: The effect of partial shading conditions on the P-V curve of an exemplary PV system [21].

Therefore, a MPPT controller is commonly added to the PV system: this device is designed to continuously track the MPP by the means of different algorithms, and ensure that the system keeps operating at maximum efficiency and power output[21, 23].

Hence, a solar inverter converts the direct current, produced by the PV panels harvesting solar energy, into alternating current suitable to be distributed at low voltage directly to residential buildings or businesses (in the case of small systems) or to be transmitted at higher voltage (for example by the means of a transformer) through the electrical grid [24]. Depending on the size (and consequently the system layout, as per Fig. 7), inverters can be classified in three categories [25]:

- Central inverters, receiving all the DC current from the PV system; these devices tend to be heavy and bulky, as they handle a high-power capacity; they also tend to be at a higher price point than smaller inverter models, and therefore are mostly utilised in large scale applications. In the park layout resulting from using these devices, all the PV panels are connected to a single inverter rated at total capacity.
- String inverters, where the PV farm is divided into several “strings” or “arrays” of solar panels connected in series, and each string is connected to a separate inverter; this is the most common layout in medium-to-large scale PV systems. In such a layout each PV array is connected to a string inverter rated at the power capacity of the PV string/array.
- Module inverters (or micro inverters) are connected to the single solar modules, providing optimisation through maximum power-point tracking for each PV module.

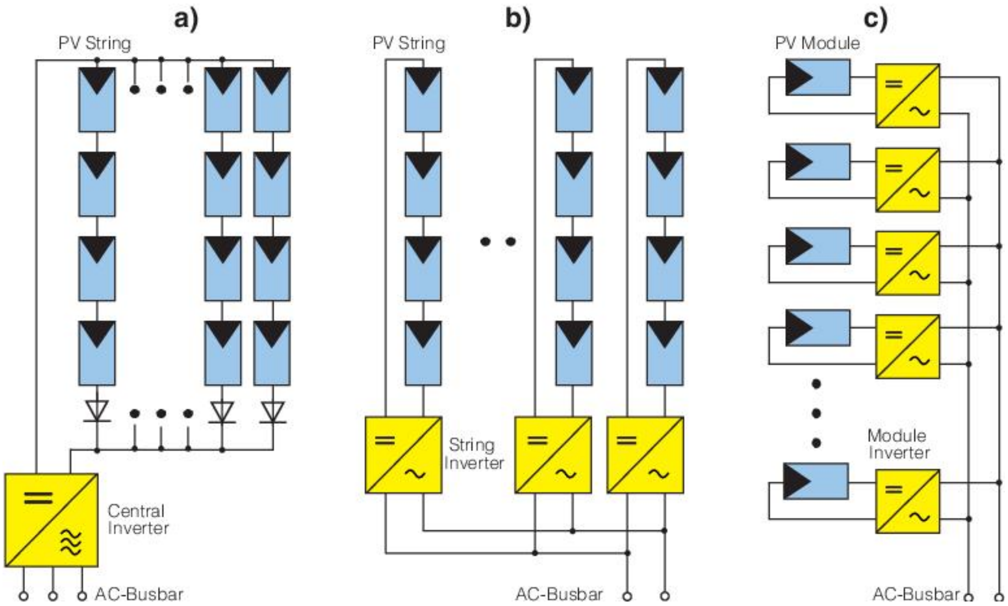

Fig. 7: Different PV system layouts depending on the inverter type: a) all the PV strings are connected to a central inverter, b) each string is connected to a separate string inverter, c) each PV module is connected to a single module inverter [26].

2.4 Power transformers

Commonly, to connect a solar PV system to an AC electrical grid, transformers are used: such devices serve the purpose of converting the value of AC voltage to a higher amount (in case of step-up transformers) or a lower amount (for step-down transformers). Normally, step-up transformers are utilised to stabilise and increase the value of the output voltage from the inverters to match the connection requirements and prepare the solar electricity for transmission into the electrical grid [27].

These devices operate by utilising the principles of electromagnetic induction: they are composed by two or more coils (or windings) wound around a common core made of laminated steel, where the magnetic field generated by the "primary" coil (receiving the input voltage) induces a voltage in the "secondary coil", resulting in the transformed output voltage. The ratio between the input and output voltage is determined by the number of turns in each coil. In standard applications for connection with the transmission grid, three-phase transformers are used, which are composed by three couples of primary and secondary windings [28-30].

Typically, they are classified depending on the medium utilised for keeping the temperature of the device under control: "dry" type transformers use air as cooling medium, utilising a vacuum pressure impregnation in epoxy or cast resin; "oil" type transformers, instead, are immersed in an oil solution that acts as a coolant as well as insulation and protection [31]. In particular, in order to prevent fire hazards and environment contamination, recently effort is being made in switching to natural ester fluids using as coolant, replacing "traditional" mineral oil derived from petroleum [32].

Both inverters and transformers are subjected to a highly variable load due to the fleeting nature of solar irradiation: as the overall output of the PV panels varies significantly depending on the environment temperature, eventual shading and daylight duration, particular consideration needs to be made in the design of the power electronics so that additional losses are limited and damage to the system is avoided [27].

2.5 Harmonic filters

Harmonics are defined as the part of a signal whose frequencies are multiples of the system's fundamental frequency: in case of sinusoidal voltage and current (such as in the case of AC), waveforms with high harmonic content will deviate from the ideal sine-wave shape, appearing distorted by the superposition of waves at different higher frequencies. Such harmonics are generated by non-linear loads, typically produced by equipment switching at high frequency (such as inverters). High harmonic content in the voltage and current signals can produce accentuated losses as well as damage to the electrical equipment and safety hazards, hence the creation of safety guidelines [33].

In order to contrast the issue of harmonic content, harmonic filters are utilised: these are resonant circuits (in series or parallel), tuned to appropriate frequencies and designed to limit or block harmonics [34].

Commonly, filters are classified into two categories: passive and active. Passive filters are composed of reactive components (such as inductors, capacitors, and resistors) tuned to undesirable harmonic frequencies by providing low impedance paths at such frequencies. They are relatively inexpensive when compared with active filters but are subjected to potential issues including interactions with the power system, compensating a limited number or harmonics, and forming parallel resonance with the system resulting in worsened power quality conditions. Active filters, instead, implement active power conditioning to eliminate harmonic currents: they utilise power electronics switching devices to detect the distortion of the load current sine wave and to correct such distortion by injecting harmonic currents with complementary magnitudes, phases and frequencies, so that the harmonic currents result cancelled out. They have the advantage over passive filters to respond effectively also in the case of changing loads and harmonic variations, but at a higher cost [35-37].

3. Method

The execution of this project can be divided into two main segments: the first step was to execute a literature research, in order to investigate the challenges and requirements related to using power electronics in floating photovoltaic parks, as well as identifying suitable models of inverters and transformers for the application considered; afterwards a simulation in PSCAD software of an exemplary model of FPV farm was performed, in order to further examine challenges, issues and possible mitigations related to the proposed system.

3.1 Literature analysis: standards and guidelines for FPV parks

As at the current time of the analysis there is no official industry standard directed at providing norms for the design and implementation of floating PV stations, it becomes necessary to identify some guidelines to follow to answer questions such as:

- What is the recommended level of protection against external environment and vibration for the inverters and transformers deployed for FPV use?
- Are there any specific certificates that these devices should comply with to be utilised in such applications?
- Is there any type of transformer (dry, oil/ester) that should be preferred for deployment on FPV stations?

After a brief analysis, two resources were identified as possible guidelines sources: the “Where Sun Meets Water” handbook by the World Bank Group [38] and the “Design, development and operation of floating solar photovoltaic systems” recommended practice guide by the Norwegian consultancy firm Det Norske Veritas, commonly known as DNV [39]. Since the former (although covering several aspects including site identification as well as financial and environmental considerations) does not provide specific enough guidelines for the electrical equipment to be used, the latter has been utilised as the main source of standards for this study. According to that, several requirements have been defined for the development and deployment of FPV parks and have been used as reference on the simulation part of this project [39].

3.2 Grid connection requirements and standards

Aside from the guidelines defined in the previous section, several standards have to be followed to ensure that the power delivered by a photovoltaic park meets the safety requirements and regulations to be transmitted through the electrical grid.

Through this study the electrical standards IEEE 519-2014 (Recommended Practice and Requirements for Harmonic Control in Electric Power Systems) and EN 50160 (Voltage Characteristics of Public Distribution Systems) were considered in order to evaluate the performance of the system.

Such standards define technical specifications and guidelines to determine if the power delivered by the system is suitable to be conducted through the electrical grid; in particular, for this study the limits regarding maximum and individual harmonic content were particularly relevant, as to determine if the voltage and current generated by the system would not exceed the recommended harmonic content. Although these standards could be applied to every segment of the electrical connection within the FPV park, including between the PV modules and the inverter(s), the focus of this analysis has been to examine the harmonic content at transformer input and at Point of Common Coupling (PCC).

According to the IEEE 519-2014 and the EN 50160, the following requirements apply: for the voltage, the IEEE 519-2014 standard recommends all the individual harmonic to be below 3% and the total harmonic distortion (THD) to be below 5% for systems rated between 1 kV and 69 kV [40], meanwhile the EN 50160 recommends specific limits for each individual harmonic (in particular, the limit for the third, fifth and seventh harmonics are set at 5%, 6% and 5% respectively) [41, 42]; for the current the IEEE standard recommends 4% as limit value for each individual odd harmonic between the third and the eleventh and 5% as limit value for the total harmonic content [40].

In addition to the EN 50160 and the IEEE 519-2014, some other standards should be considered in reference to the connection of FPV parks to the AC grid. The IEC 62930 is the recommended standard by the DNV guidelines to define the required characteristics of the PV cabling, including parameters such as the DC rated voltage (1.5 kV), conduction material (copper), current carrying capacity and insulation resistance (dependent on the thickness of the conductor) [43]. Furthermore, DNV's recommended practice guide suggests the IEC 60364 as the standard to follow for the low-voltage, non-PV cabling and the IEC 60183 and IEC 63026 for respectively medium voltage cables installed above water and medium voltage cables installed directly under water [39].

3.3 Inverter requirements

The guidelines from DNV recommend locating both inverters and transformers on floating structures neighbouring the floating PV arrays, especially for large scale FPV parks and FPV parks located at notable distance from shore; in this case, the power electronics floating offshore will be connected via cabling to the onshore switching facilities and grid interconnection point. For smaller floating solar parks located at a shorter distance from the shore, the option of locating the power electronics converters directly on land is also accepted [39].

In terms of protection against the external environment, DNV's recommended practice guide differentiates between requirements for central inverters and for string inverters, referring to the Ingress Protection (IP) rating. Such standard is utilised to evaluate the level of resistance of an enclosure against the ingress of dust or liquids: the first numeral of the IP rating rates the enclosure's protection against solid objects, scaling from 0 (no protection) to 6 (completely sealed from ingress of dust); the second numeral, instead, refers to the protection against liquids and is rated from 0 (no protection) to 9 (protection from high-pressure hot water from different angles) [44].

According to the selected guidelines, centralised inverters installed within an enclosure are required to have enclosure rating of IP 44 or higher. In general, inverters installed on fixed platforms are recommended to be rated IP 54 or higher, with the control and power electronics to be separately encapsulated in an enclosure with at least IP 65 rating. Furthermore, adequate lightning protection and cooling systems should be incorporated in the enclosure to ensure optimal performance and safety of the inverters [39].

For string inverters, as they are likely installed directly on the PV floaters (all the models investigated had a weight below 160kg, and hence it was assumed that they could be installed directly on the floaters together with the PV modules) and therefore more subjected to the external environment than central inverters, a protection rating of IP 65 or higher is advised. Also, the ventilation design of the enclosure should consider the exposure to higher humidity and increased temperature due to direct sunlight [39].

Ideally, inverters to be deployed for floating applications should comply with several safety certifications, not only including local regulations and requirements for grid connection systems and grid monitoring, but also the following standards [39]:

- IEEE 1547 - Interconnection and interoperability of distributed energy resources with associated electric power systems interfaces;
- IEC 61000-6-2 and IEC 61000-6-4 - Electromagnetic compatibility (EMC) (Part 6-2 and Part 6-4): Generic standards, Immunity and emission standard for industrial environments;
- IEC 62920 - Photovoltaic power generating systems: EMC requirements and test methods for power conversion equipment;
- IEC 62477 - Safety requirements for power electronic converter systems and equipment;
- IEC 61727 - Photovoltaic systems - Characteristics of the utility interface;
- IEC 62109 - Safety of power converters for use in photovoltaic power systems;
- IEC 62116 - Utility-interconnected photovoltaic inverters: Test procedure of islanding prevention measures.

Concretely, looking at the offer available in Europe from the most popular producers of solar inverters, no inverter model was found to comply with all the requirements and certificates indicated by the recommended practice guide. Regarding the safety standards, some companies disclaim in the datasheet of their models that more compliance certifications are available upon request or that the certificates and approvals listed are only a selection [45, 46]. Hence, because of lack of clarity regarding the availability of inverters fully complying with the recommended certifications, priority was given to identifying models with suitable IP protection while complete compliance with all the IEEE and IEC standards was not held as a mandatory prerequisite when selecting suitable models through this study. The selection of models deemed suitable was then used to determine the characteristic of the inverter used in the simulation.

3.4 Transformer requirements

For transformers, the recommended prerequisites from the guidelines include casing with an IP 44 rated (or above) ventilated enclosure and compliance with IEC 60076 [47]. Also, it is in general advisable to utilise dry type transformers for floating solar applications, especially in the case of the installation site being subjected to high waves and/or strong winds, or the water body being utilised for commercial fishing or as drinking water source; if an oil type transformer is deployed instead, it should be a model with natural oil or natural ester fluids, and maximum attention should be given in order to minimise the risk of oil spillage and leakage [39].

3.5 Choice of PV panel model for the simulation

To examine in detail the potential and challenges related with a large floating photovoltaic park, the PSCAD software was used to design and simulate the operation of a model of such a park. This software was chosen to align with other parallel student projects, and to keep open the possibility for future transient analysis. The PV modules used as reference for this study were the "Vertex Backsheet DE21" solar panels from TrinaSolar [48], to align with related studies on the topic [49]. This module is composed by PERC cells, providing high power and efficiency ratings, and resulting in the following technical specifications (Table 1, Fig. 8, Fig. 9):

Table 1: Trina Solar "Vertex Backsheet DE21" module technical data [48].

Characteristic	**Value**
Maximum power output	670 W
Maximum efficiency	21.6%
Maximum power voltage	38.2 V
Maximum power current	17.55 A
Open-circuit voltage	46.1 V
Short-circuit current	18.62 A
Number of cells	132 cells
Module dimensions	2384×1303×35 mm
Weight	33.6 Kg

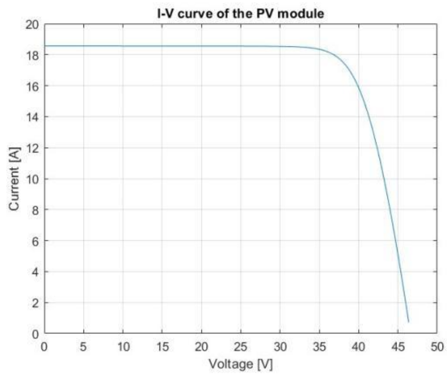

Fig. 8: Current-Voltage (I-V) curve at 1000 W/m^2 irradiance value for the Trina Solar "Vertex Backsheet DE21" module [48].

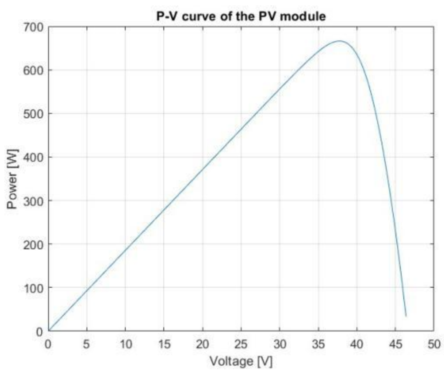

Fig. 9: Power-Voltage (P-V) curve at 1000 W/m^2 irradiance value for the Trina Solar "Vertex Backsheet DE21" module [48].

3.6 Complete park layout

A partial system layout including the "scaling component" is illustrated in Fig. 10, while Fig. 11 displays the whole system represented by the PSCAD simulation.

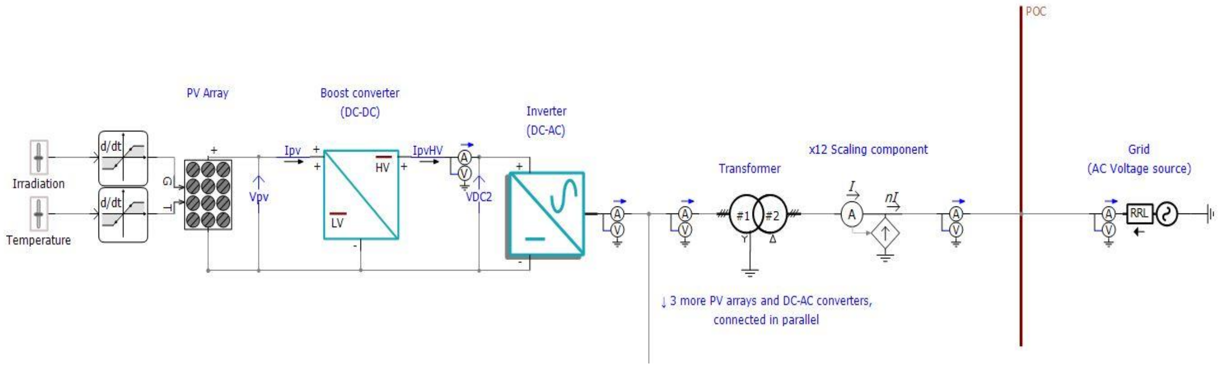

Fig. 10: Partial system layout of the PSCAD simulation (not including the additional three branches composed of PV array and inverter). The complete layout is shown in Appendix A.

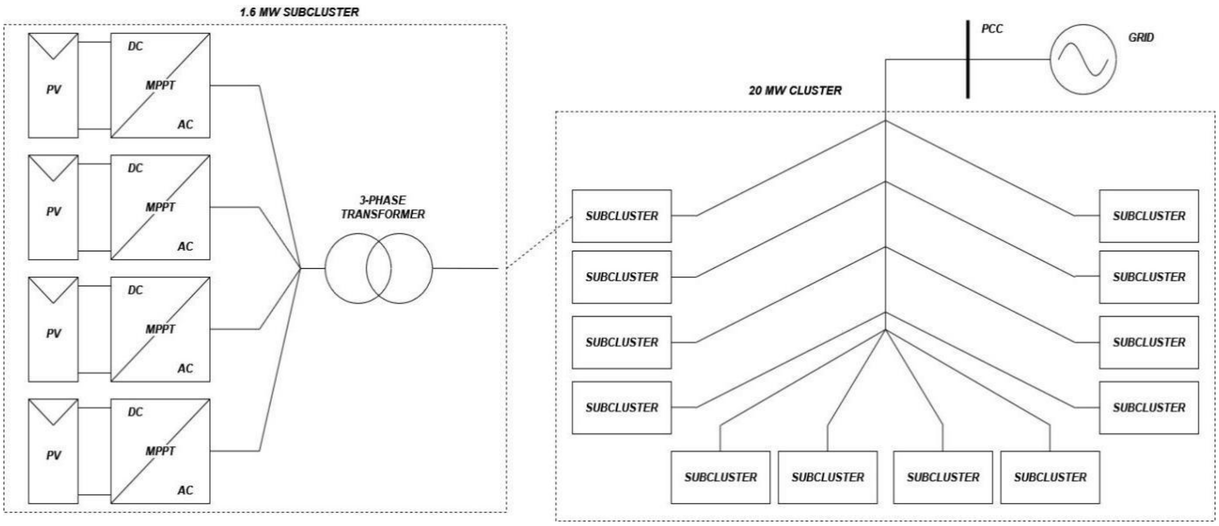

Fig. 11: Schematic of the system simulated on PSCAD (own diagram).

Potentially, this design in sub-clusters and clusters allows the system to be scaled further, simulating power plants of much larger scale and investigating the operation of FPV parks reaching even 1 GW rated power: in such case, the cluster of 20 MW presented in Fig. 11 should be paired to other identical clusters for a total of 50 clusters rated at 20 MW and connected in parallel to the grid, resulting in a total of 1 GW power production.

The entire layout, the different system components, and the sizing of the system are described in detail in the following sections.

3.7 Choice of layout for the simulation

The objective of the simulation was to analyse the operation of an OFPV plant characterised by power capacity ranging between 10 MW and 50 MW, with the power plant divided in "clusters" of smaller power capacity choosing between two layout options:

- Cluster layout with central inverters, as presented in section 2.3 in Fig. 7;
- Cluster layout with several string inverters, as presented in section 2.3 in Fig. 7.

For this analysis, the layout utilising string inverters was chosen, as most of the available options are string inverters (as per the analysis results, presented in section 4.1 and Table 7) and as this choice of layout does not require additional analyses for the weight carrying capacity of floaters and for the eventual need of specially designed platforms.

Hence, the Sungrow "SG350HX" was chosen as the string inverter model of choice for the PSCAD simulation, as it provides relatively high-power capacity for a contained weight, as well as being rated with a high protection against the external environment and being suitable for connection with the solar modules from Trina Solar. The electrical specifications for the inverter used in the PSCAD design have been retrieved from the datasheet of this model [50] and listed in Table 2.

Table 2: Electrical specifications for Sungrow's "SG350HX" inverter model [50].

"SG350HX" inverter electrical specification	**Value**
DC input voltage range	500 V - 1500 V
Max DC input current	480 A
Max AC output power	352 kW
Max AC output current	254 A
AC output voltage range	640 - 920 V

Regarding the transformer selection, the "Siltrim" model from Schneider Electric was chosen as reference since the information about its electrical and technical specifications was readily available and its rating matched connection with the chosen inverter model from Sungrow. The electrical data for this transformer model are listed in Table 3.

Table 3: Electrical specifications for S.E.'s "Siltrim" transformer model [51].

"Siltrim" transformer electrical specification	**Value**
Rated power	1.6 MW
Rated low voltage	690 V
Rated high voltage	20000 V

From these data it was possible to determine the appropriate configuration and layout of the system for the PSCAD simulation. As the transformer is rated 1.6 MW, that was also determined as the cluster power capacity. Given this rating, four inverters could be connected in parallel to the transformer, resulting in 1.408 MW of rated power from the inverters, as

$$352\ kW \cdot 4 = 1.408\ MW$$

The total power capacity from the inverters did not reach the rated power of the transformer, to guarantee safe and proper functioning of the transformer and avoid damages to the equipment in case of power spikes or malfunctioning from the inverters.

Hence, the system resulted in four PV arrays, each connected to an inverter, and then all the four inverters connected in parallel to a transformer. As each inverter was rated at 352 kW power capacity, that was taken as the max output power from the PV array, resulting in a PV array composed by

$$352\ kW_{inverter} \div 670\ W_{PV\ modules} = 525\ PV\ modules$$

As 525 modules rated at 670 W would provide 351.75 kW of maximum output power.

Also, as the max input voltage for the inverter is 1500 V (Table 2) and the open circuit voltage from each PV module is 46.1 V (Table 1), the maximum number of PV modules connected in series in the PV arrays was 32. Similarly, as the max input current for the inverter is 480 A (Table 2) and the short circuit current from the PV modules is 18.62 A (Table 1), the maximum amount of PV modules in parallel in the PV arrays was determined to be 25.

The chosen design for a PV array composed by 525 PV modules (and respecting the limits of max open output voltage and max output current) was 25 rows of PV panels (connected in series) and 21 strings (parallel connection), resulting in

$$46.1\ V \cdot 25\ rows = 1152.5\ V_{max\ OC\ voltage}$$

$$18.62\ A \cdot 21\ strings = 391.02\ A_{max\ SC\ current}$$

Thus, the resulting PV arrays were each composed of 525 PV modules, 21 in parallel and 25 in series, for a total rated power of 351.75 kW per array. Furthermore, it was noted that in order to deploy this design in FPV applications, the PV array considered could be divided into 75 floating clusters of 7 PV modules each, for a power rating of 4.69 kW for each floater.

3.8 PV modules and PV array

From the previous calculations it was possible to determine the overall layout of the system. The PV panels in the PSCAD simulation were modelled taking the previously mentioned "Vertex Backsheet DE21" solar panels from TrinaSolar [48] as reference, whose characteristics have been enunciated in Table 1.

For every solar array, the PV panels were connected via cabling in 21 parallel strings, each composed by 25 PV modules connected in series, resulting in an array characterised as follows:

Table 4: Design details of each PV array in the PSCAD simulation.

PV array characteristic	**Value**
Number of PV modules	525 modules
Modules in series	25 rows of modules
Modules in parallel	21 strings of modules
Rated power	351.75 kW
Max output DC voltage	1152.5 V
Max output DC current	391.02 A

This layout provided the power curves illustrated in Fig. 12 and Fig. 13. Such curves display how the PV array properly scales the characteristics of the modules shown in Fig. 8 and Fig. 9, as presented in 2.2.

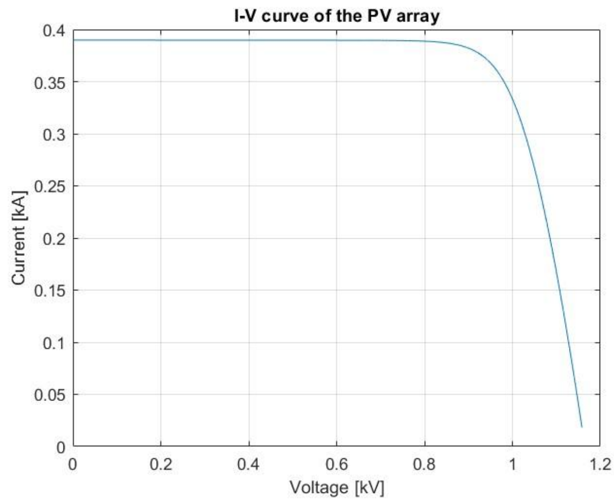

Fig. 12: Current-Voltage curve of a single PV array in the PSCAD design.

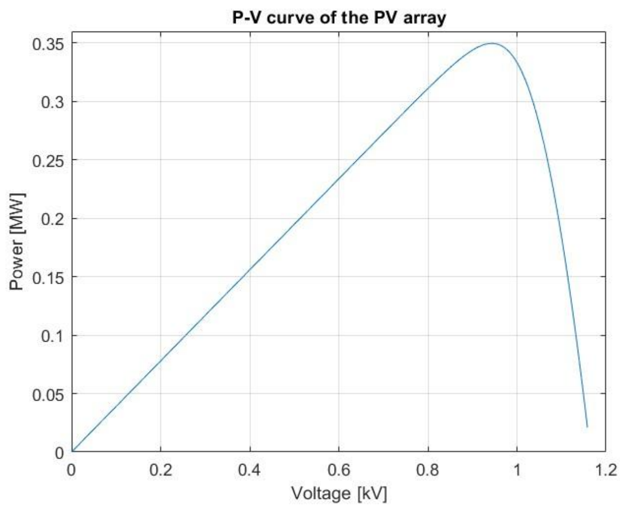

Fig. 13: Power-Voltage curve of a single PV array in the PSCAD design.

Hence, each of the PV arrays was wired to an inverter, modeled after the "SG350HX" model from Sungrow [50], whose characteristics have been listed in Table 2. Thus, the following electrical specifications were applied to the PSCAD design of the inverter:

Table 5: Electrical data of each inverter in the PSCAD simulation.

Inverter characteristic	Value
Rated input DC voltage	1500 V
Max input DC current from PV	480 A
Rated AC output power	352 kW
AC output voltage (RMS)	690V

3.9 Inverter and control loops

Each inverter was modelled as two components, a DC-DC boost converter and the actual DC-AC inverter (or voltage source inverter - VSI). The purpose of the DC-DC converter was to modify and set the value of the DC input of the inverter, in order to ensure operation at MPP (as enunciated in section 2.3). A simple control loop (Fig. 14) was connected to the boost converter with this purpose: based on the reference power generated by the maximum power point tracker, the converter adjusts its output current "IpvHV", which is fed to the DC-AC inverter (Fig. 10).

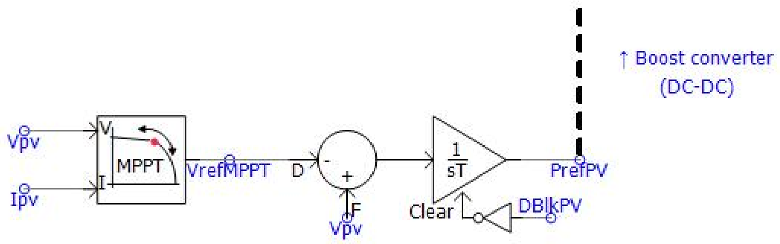

Fig. 14: Control loop determining the MPP tracking of the boost converter, where I_{PV} and V_{PV} are respectively the output current and output voltage from the solar array, used as reference to determine the MPP.

The boost converter with its components is displayed in Fig. 15. The controller is exposed in Fig. 16: the reference power is compared to the DC link power, and the error signal is forwarded to a PI controller to generate the DC-DC converter duty cycle.

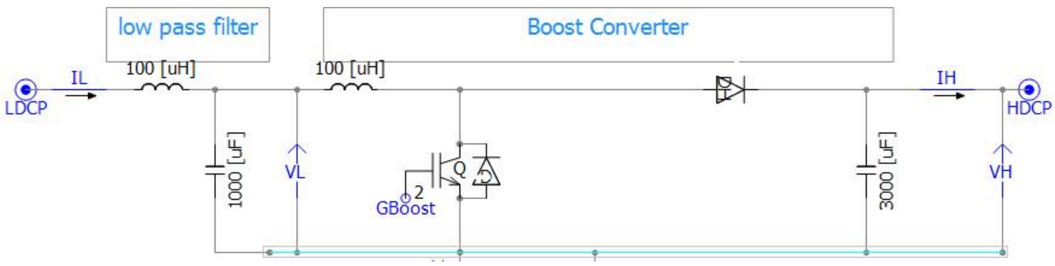

Fig. 15: Components of each DC-DC converter in the PSCAD simulation.

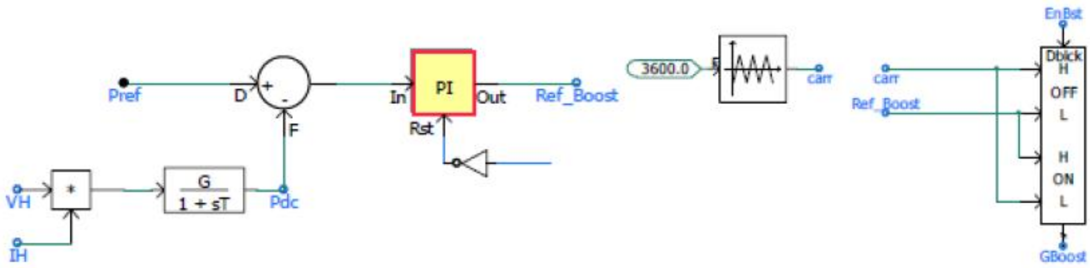

Fig. 16: The power controller of each DC-DC converter.

The VSI component was designed as a three-phase inverter composed of a DC link consisting of two capacitors and six IGBT switches, as illustrated in Fig. 17.

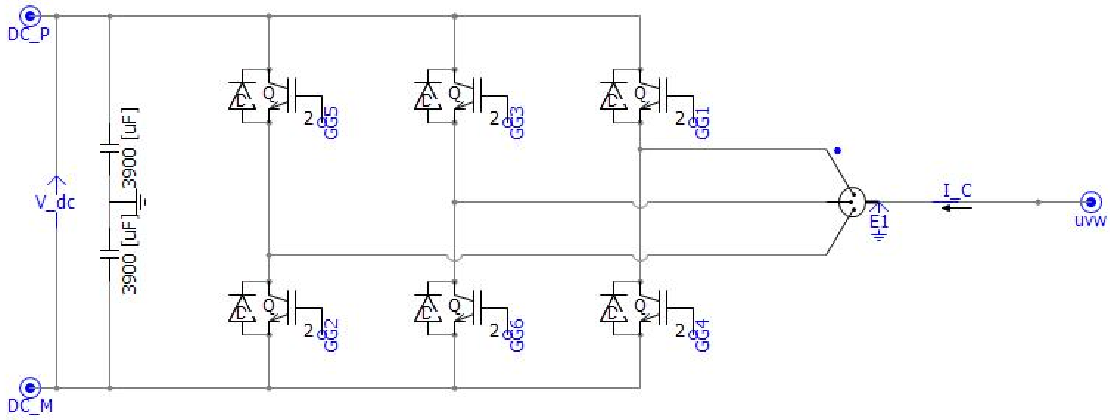

Fig. 17: Components of each DC-AC inverter in the PSCAD simulation.

The switching action of the VSI was controlled by utilising a phase-locked loop (PLL) in order to generate PWM reference waveforms while controlling the DC voltage and the reactive power, as per Fig. 18-21.

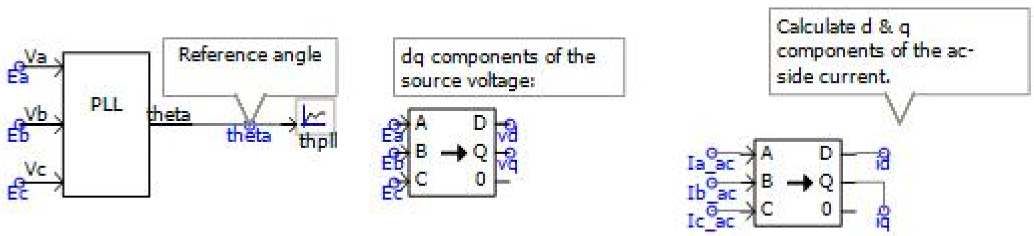

Fig. 18: PLL reference frame.

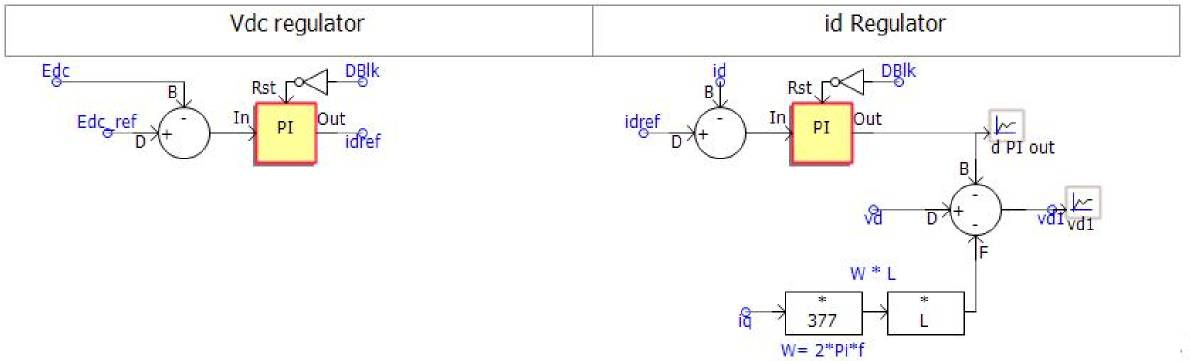

Fig. 19: DC voltage controller of the inverter.

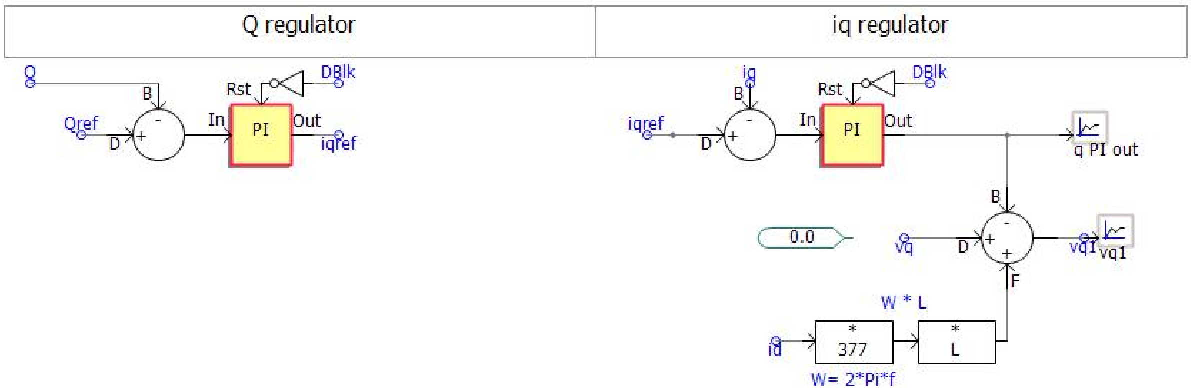

Fig. 20: Reactive power controller of the inverter.

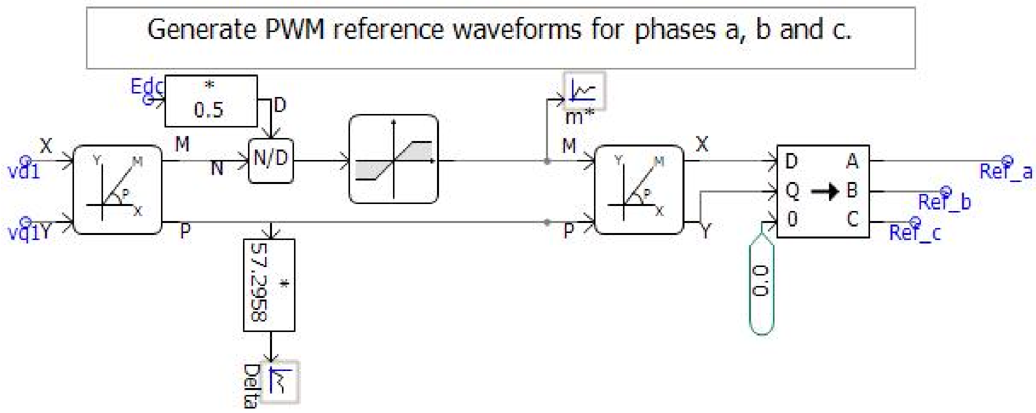

Fig. 21: PWM reference waveforms generation for the inverter control.

3.10 Harmonic distortion calculator

The THD was calculated by means of Fast Fourier Transform (FFT), so that each three-phase signal was sampled and decomposed into harmonic constituents to be fed to the harmonic distortion calculator (Fig. 22).

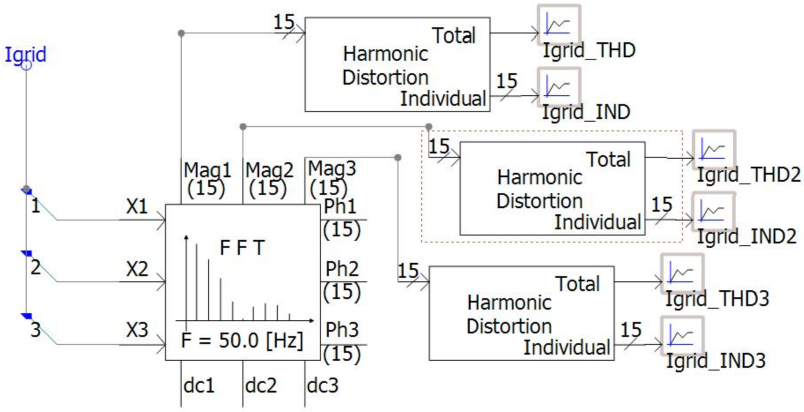

Fig. 22: The three-phase grid current signal being decomposed in the harmonic components of its phases, and then calculating the individual and total distortion for each phase.

On the PSCAD simulation, the FFT block utilises a "sliding window" to analyse segments of the input signal and provide the harmonic magnitude of such segment as output: in such way it was possible to calculate and examine how the THD of different signals changed and evolved during the course of the simulation, and plot it in the time domain. The frequency for the moving window was set to 50 Hz, hence analysing the signal in segments of 0.02 seconds.

3.11 Harmonic filter design

In order to mitigate the THD, several different designs of passive harmonic filters were considered:

- Single tuned filters (or series filters) are designed to target only one specific harmonic frequency, and are composed by a series resonant circuit consisting of a capacitor, an inductor and a resistor [52];
- High pass filters utilise a resistor and an inductor in parallel connection and a capacitor connected in series, and target higher order harmonics above a certain cut-off frequency determined by the values of the resistance and the capacitance. They are mainly used to eliminate harmonics of fifth order or higher [52];
- Bandpass filters (or double tuned filters) are a combination of two series filters, and are also designed for higher harmonic filtration, commonly targeting two specific harmonic frequencies [52];
- C type filters are designed to target low order harmonic frequencies, such as the second or third harmonic. They consist of two capacitors, an inductor and a resistor [52];
- L, LC and LCL type filters are among the most common types used to filter the harmonics produced on the AC side of inverters. L filters are the simplest ones, being composed only by a single inductor, but are also characterised by low efficacy in attenuating harmonics, hence requiring a high filtering inductance. LC filters are composed by an inductor and a capacitor, providing enhanced harmonic suppression at lower inductance values when compared with L filters. Finally, LCL filters provide the best harmonic attenuation of the three types and are composed by two inductors and a capacitor. However, this type of filter is prone to resonance and other potential issues such as current ripple through the inductors. The design of these three types of filters is presented in Fig. 23 [53].

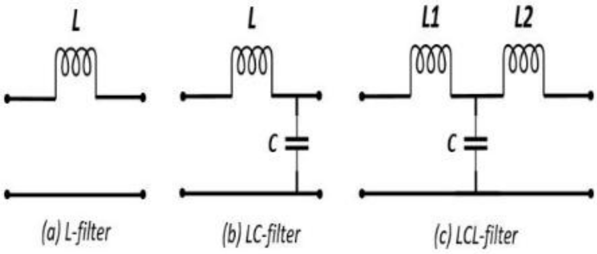

Fig. 23: Design of a) L filters, b) LC filters, c) LCL filters [53] (© IEEE 2019).

For the scope of this project it was determined that LCL filters should provide the highest efficacy compared to other passive filters [54-56], as they are specifically designed to reduce switching frequency harmonics caused by power converters [57]. As illustrated in Fig. 23, such filters are designed by connecting two inductors (L1 and L2) in series and a capacitor (C1) between them in parallel. However, this topology of filters also introduces instability and oscillation problems due to resonance [54, 56]; hence, the addition of damping components to the filters becomes fundamental, to limit these resonance effects [54, 56, 58]. In particular, the split-capacitor resistive-inductive (SC-RL) passive damping scheme appears to be the most efficient [58] and was the one utilised through the software simulation part of this project; such damping is carried out by adding a capacitor, a resistor, and an inductor in parallel to the capacitor of the LCL filter (Fig. 24).

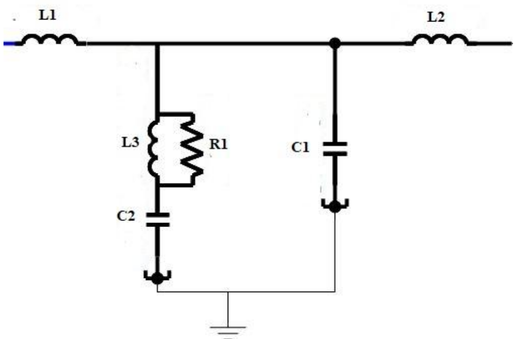

Fig. 24: Design of the SC-RL damped LCL filter (from own PSCAD simulation).

3.12 Cabling

In the PSCAD software the connecting lines simulating the cabling are by default modeled as ideal conductors. Hence, a brief analysis providing a rough estimation for cabling losses has been executed separately and presented in section 4.9.

3.13 Organisation in subclusters and clusters

In total, in the PV park model four "lines" (composed by PV array, DC-DC converter, inverter and connecting wires) were connected in parallel, for a total output of 1.408 MW at 690 V output AC voltage. These were then connected to a transformer modelled following the characteristics of the "Siltrim" model from Schneider Electric [51], the characteristics of which were listed in Table 3. Thus, the transformer designed in PSCAD had the following specifications:

Table 6: Electrical data of the transformer in the PSCAD simulation.

Transformer characteristic	**Value**
Rated power	1.6 MW
Input Low AC Voltage (RMS)	690 V
Output High AC Voltage (RMS)	20000 V (20 kV)

The transformer was followed by a “scaling component” with the purpose of scaling the system and simulating a large-scale park, composed of several “clusters” and “sub-clusters” of the same system. Hence, the system before the “scaling component”, at 1.408 MW power rating from the inverter, 1.6 MW rated power from the transformer and 20 kV AC voltage level, is considered as a “sub-cluster”. In order to simulate a larger cluster, the PSCAD “scaling component” was introduced with a scaling factor of 12, simulating 12 of such sub-clusters connected in parallel and resulting in a cluster of around 20 MW rated power (concretely, 17 MW was the resulting rated power from the solar park). Finally, the system was connected to an AC source simulating the electrical grid, with voltage at PCC of 20 kV and 50 Hz frequency.

4. Results

4.1 Suitable inverter models

According to the requisites and assumptions mentioned in sections 3.3 and 3.4, an investigation of the main providers of power conversion devices for solar application was made to find suitable models to be deployed on OFPV parks. For inverters, the following were found appropriate, as displayed in Table 7 (note: the following results do not claim to provide an exhaustive summary of all the devices in the market compliant with the guidelines introduced previously, but rather to showcase a selected sample of suitable models for the European market at the time that this analysis was made):

Table 7: Selection of suitable inverter models.

Brand	Model	layout	rated power [kW]	IP rating	weight [kg]	source
FIMER	PVS-175-TL	string	175	IP 65	153	[59]
FIMER	PVS980-58	central	5000	IP 55	6000	[60]
Huawei	SUN2000-115KTL	string	125	IP 66	93	[61]
Huawei	SUN2000-90KTL	string	100	IP 65	80	[61]
Power Electronics	HEM-IEC	central	4200	IP 55	14000	[62]
Power Electronics	HEMK	central	4390	IP 55	5500	[63]
SMA	Sunny	central	1980	IP 65	3400	[64]
SMA	Sunny up	central	3680	IP 54	3700	[64]
SMA	Tripower	string	110	IP 66	94	[64]
Sungrow	SG110CX	string	110	IP 66	89	[65]
Sungrow	SG125CX-P2	string	125	IP 66	87	[65]
Sungrow	SG350HX	string	352	IP 66	116	[65]

For this analysis and for the purpose of selecting models to use as reference when designing the system in PSCAD, the weight limit for the inverters has been assumed to be at 4 tonnes in order to be deployed in offshore floating photovoltaic applications. Realistically, the specific weight limit and the choice of inverter will depend on the characteristics of the installation site and structures utilised, and whether fixed elevated platforms for power conversion equipment are included. This assumption mainly affected the selection of suitable central inverter models, resulting in the "PVS980-58" model of central inverter from FIMER and the two models from Power Electronics being excluded from the candidate selection.

Realistically, the selection of which model of power electronics inverter to utilise for the design and implementation in a floating PV farm will depend on several factors: from the size of the park and its power capacity to the layout and disposition of the panels as well as their power rating, the size of the floaters and weight capacity, economical convenience, and so on.

4.2 Suitable transformers

For transformers it was much more challenging to obtain detailed technical data as the publicly available information is very limited, and most companies tailor their offer to the specific needs of their client's scope. Overall, in the limited time period of this project it was not possible to find a dry type of transformer model for which its datasheet would be publicly available, meanwhile fitting the IP rating and certification compliance requirements. Because of that, priority was given to finding models with detailed technical information available to the public, and as close as possible to the specifications described by the selected guidelines. In more detail, the following seemed eligible sources to find information about transformers suitable for FPV applications:

- Hitachi Energy offers "OceaniQ", which appears to be a portfolio of solutions and products for the offshore segment that includes transformers for offshore substations, floating applications, and for offshore wind turbines [66];
- SGB-SMIT Group claims to deliver dry-type cast-resin transformers up to 25 MVA and 40.5 kV rating, protected against salty air and resistant to vibration [67];
- WEG also claims to offer dry-type transformers with minimum environmental impact, suitable for offshore applications [68];
- Schneider Electric (S.E.) was the only brand already providing technical data for the models examined, even though usually not including information relative to IP rating and compliance with the IEC 60076 standard [69]; aside from their dry type transformers, also their oil-immersed "Siltrim" model seemed suitable for floating PV farms, as S.E. declares that it's designed for renewable energy application both offshore and onshore, as well as being fire resistant [51];
- Finally, some research papers also provide data, specifications, and design implications for solar transformers to be integrated into large scale solar farms [70-72]; however, currently no literature was found to specifically focus on floating solar implementations.

4.3 Simulation details

The project on PSCAD simulates 20 seconds of power plant operation, allowing the system to overcome the initial oscillations and reach steady state. Different solar irradiation values were considered, while the ambient temperature was set at 25° C. In the simulation several parameters were monitored in order to adequately examine the performance of the solar park model: from the active and reactive power delivered to the grid by the whole cluster and by the single PV array, to the different output voltage and current levels, and most importantly the level of harmonics released from the inverters and from the transformers.

Such examination was performed following different sub-cases, to thoroughly investigate the performance of the PV plant model under different conditions; hence, the following analyses were made:

- Comparing the system operation between the case of a "strong" electrical grid (characterised by 250 MW power rating and 80 degrees of impedance angle) and of a "weak" grid (50 MW power, 10 degrees impedance angle), while keeping standard test conditions (STC, that is 1000 W/m^2 of solar irradiance and 25° C ambient temperature);

- Analysing its performance for different irradiance values (1000 W/m^2 as per STC, exaggerated rate of 1100 W/m^2, reduced rate of 850 W/m^2);
- Investigating the repercussions on the system in the case of a PV array subjected to different irradiance from the others (simulating for example the case of a passing shadowing object), while the rest of the PV arrays are kept at STC.

4.4 Simulation with no filter added

The first analysis performed on PSCAD included running the simulation at STC (1000 W/m^2 irradiance, 25° C temperature) without adding any harmonic filter to the system, to see how it would perform. Also, for this first analysis the grid characteristics were set to simulate a "strong" grid, with 250 MW power rating and 80 degrees of impedance angle.

As expected, the switching equipment included in the inverters induced a significant number of harmonics in the model (with peaks above 100% total harmonic distortion), together with other major power quality issues. Even in the last second of the simulation the model did not reach a steady state and both the voltage and the current on the grid side presented significant oscillations and disturbances. Furthermore, both active and reactive power were drawn from the grid, resulting in highly irregular power curves, as per Fig. 25-28.

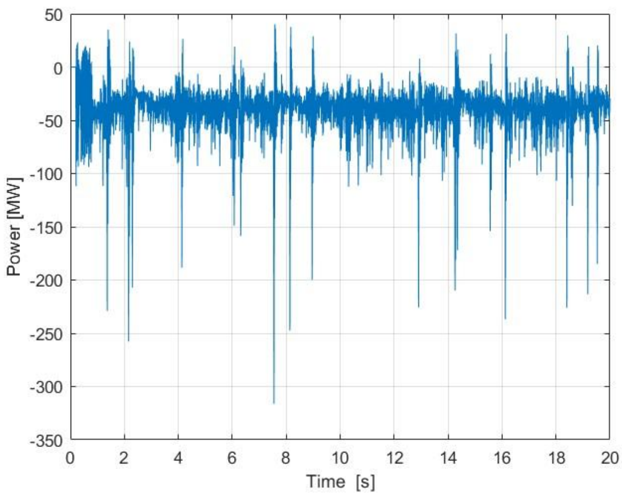

Fig. 25: The curve of the active power on the grid side during the simulation without harmonic filters.

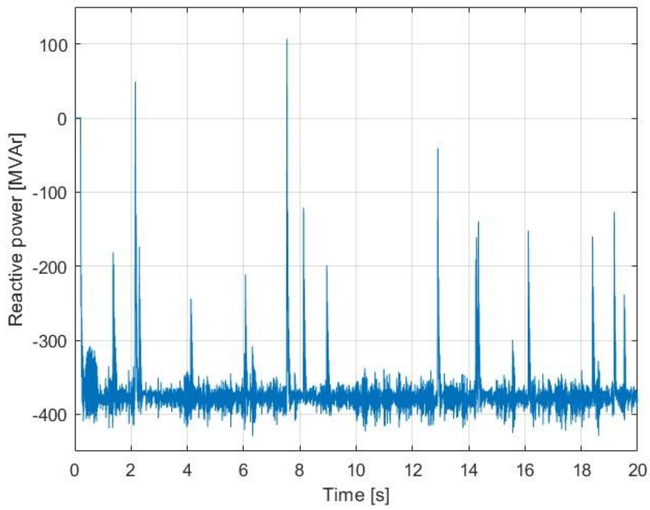

Fig. 26: The curve of the reactive power on the grid side during the simulation without harmonic filters.

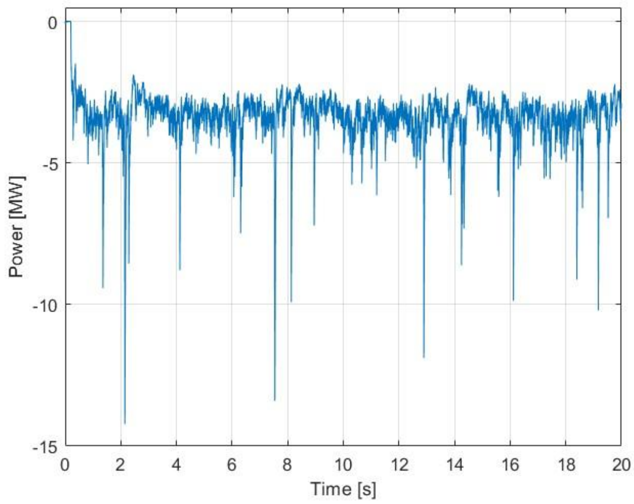

Fig. 27: The curve of the active power at the transformer's input during the simulation without filters.

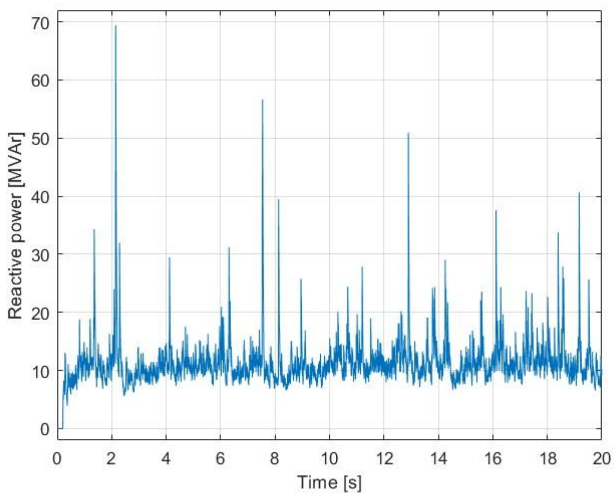

Fig. 28: The curve of the reactive power at transformer's input during the simulation without filters.

As visible in Fig. 25 and Fig. 27, the park overall drew active power from the grid (with the exception of a momentary few peaks). In particular, the average active power at PCC was determined to be around -41 MW meanwhile the average reactive power was around -369 MW, for a total of around -410 MW of apparent power drained from the system. Considering that each PV array was rated at peak power 428.8 kW in STC (as calculated in section 3.6) and that the overall PV park in the software simulation was composed by 12 subclusters each composed by four arrays, for a total of 48 PV arrays (as per section 3.9), the theoretical total peak power delivered by the PV panels amounted to around 20.6 MW. Hence, in this simulation the system was dissipating more than the sum of the theoretical total power delivered by both the PV park and the 250 MW from the grid. This could be caused by several factors: for example, it could be that the excessive harmonic content caused instability and resonances which resulted in an altered power flow and exaggerated power demand, or another possibility would be that the unfiltered harmonics in the PSCAD simulation caused unrealistic power readings and inaccuracies due to limitations of the software.

In general, the model presented extremely high harmonic peaks, a lot of oscillations and disturbances and an overall inadequacy to deliver electrical power to the grid. In particular, the following harmonic curves resulted from this simulation (Fig. 29, Fig. 30).

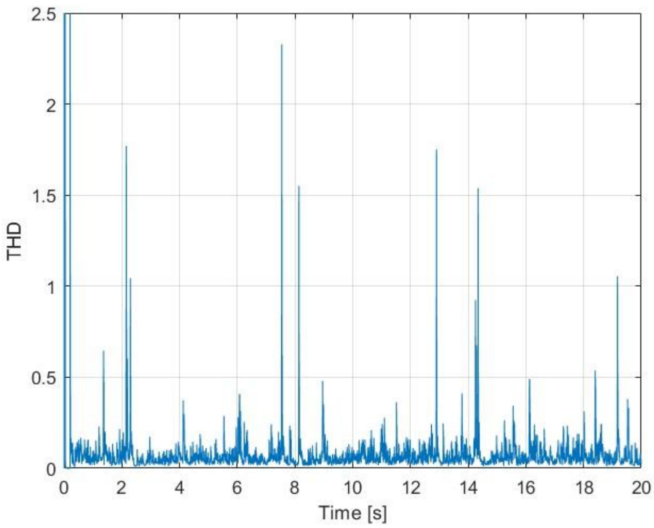

Fig. 29: The current THD on the grid side.

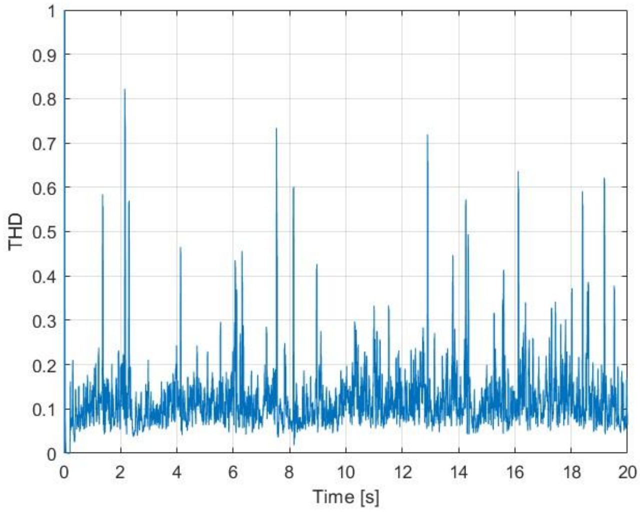

Fig. 30: The voltage THD on the grid side.

The results of this simulation, exposed in the previous figures, are summarised in Table 9. It is visible how the system didn't meet the grid requirements presented in section 3.2, as well as failing to deliver the expected 17 MW of active power.

Table 9: Results of the simulation without harmonic filters added.

Parameter	Value
Average THD of the grid current	7.5%
Average THD of the grid voltage	12.4%
Maximum THD of the grid current (omitted initial transients)	233%
Maximum THD of the grid voltage (omitted initial transients)	82.2%
Maximum amplitude imbalance of the grid current	1.23%
Average active power	-41 MW
Average reactive power	-369 MW

4.5 Filtering

The structure of the filters utilised in the simulation part of this study is the same as the one displayed in Fig. 24. Such structure enables accurate and elaborate tuning of the filter, as each component has a different influence on the filtering/damping capability of the filter.

The tuning process was executed empirically (both because of timing constraints and of lack of material providing a suitable alternative), by iteratively modifying and setting the filters parameters while tracking the harmonic attenuation. An attempt was made to include in the model layout only 1 LCL filter between the node connecting the inverters and the transformer, but that did not lead to satisfying improvements in the power delivered from the system; that was not unexpected, as it is recommended standard procedure to add an individual LCL filter after each switching power converter to obtain satisfying harmonic attenuation [73]. Hence, one filter was added after each DC-AC converter for a total of four filters, and the structure of each one of the four inverters was set as per Fig. 31.

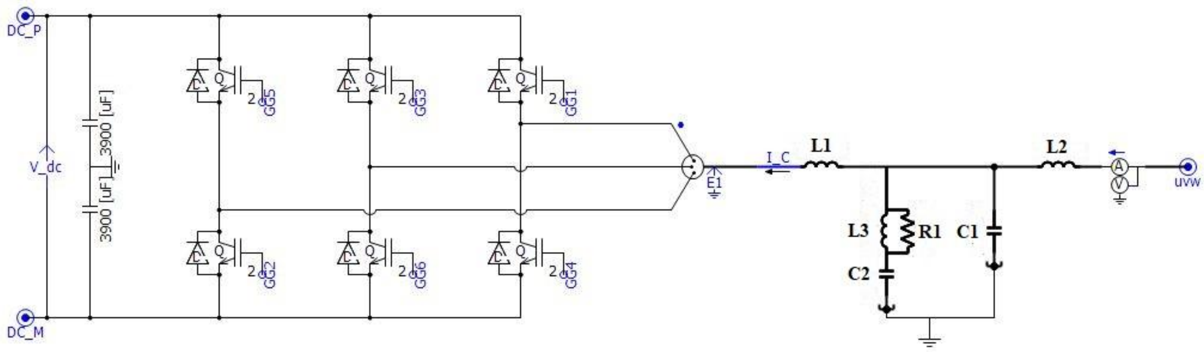

Fig. 31: The inverter with LCL filter structure used in the PSCAD model.

This modification led to significant improvements in terms of system stability, power quality and harmonic attenuation. As previously introduced, tuning the filters was necessary to maximise harmonic attenuation. This was obtained by finding the best compromise between maximising the attenuation of both low frequency and high frequency harmonics (by modifying and increasing the values of L1, L2, C1) as well as damping appropriately the filter (by operating on L3, R1 and C2), as an excessive filtering action (led by exaggerated values of L1, L2, C1) would lead to system instability and oscillations, as illustrated by the harmonic curve on Fig. 32 (compared to the harmonic curve on a more balanced system in Fig. 33).

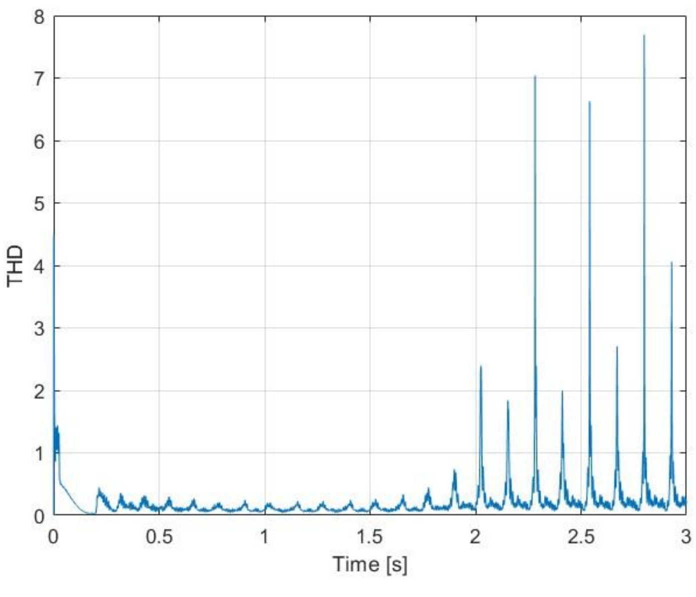

Fig. 32: Total Harmonic Distortion of the current entering the transformer in a model with overly strong filters; as visible, the damping does not prevent increasing oscillations and the system does not reach steady state. This is due to the resonance effect not being damped properly, as an unbalance between the filtering components and the damping components causes the resonance frequency to not be adequately attenuated.

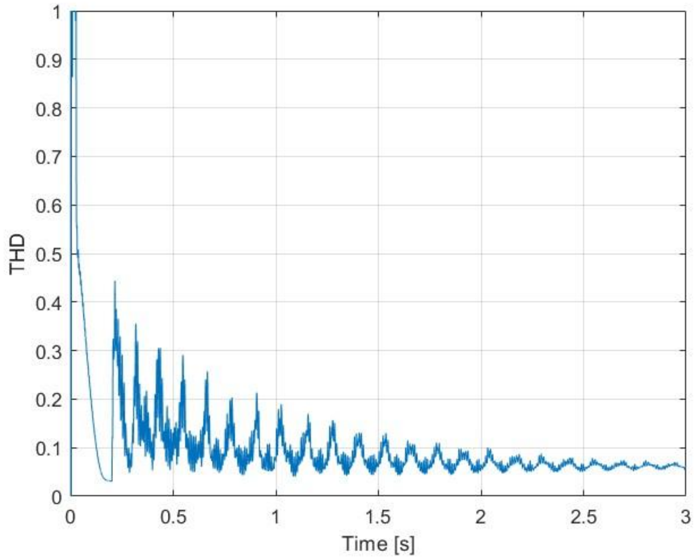

Fig. 33: THD curve of the current at transformer input in a model with balanced filtering and dampening.

The optimal values found for the filter parameters with STC and strong grid conditions are listed in the following section, together with the values obtained for the harmonic content after adding filters. Once tuned filters were added to the system (meanwhile keeping the previous conditions of STC and strong grid connection), the model finally provided proper power quality and power delivery to the grid within the expected values, as presented in the following figures (Fig. 34-39).

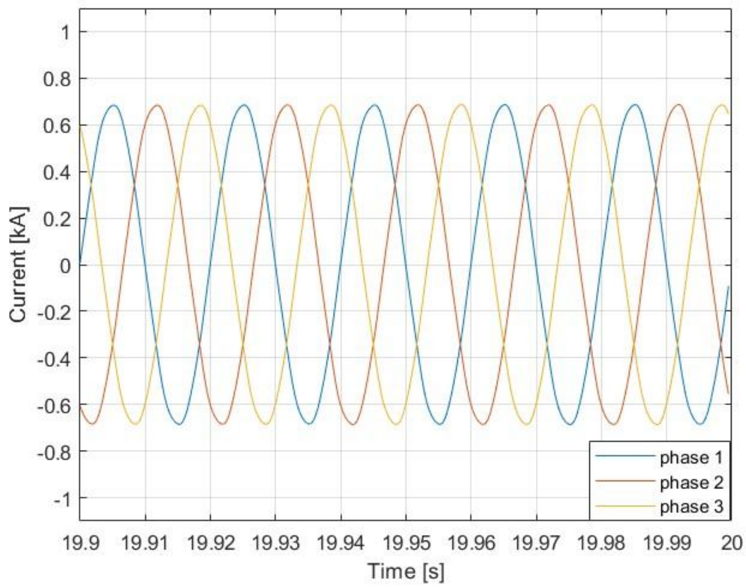

Fig. 34: The grid current at the end of the simulation with harmonic filters added; the curves presented a consistent sinusoidal shape with balanced phases.

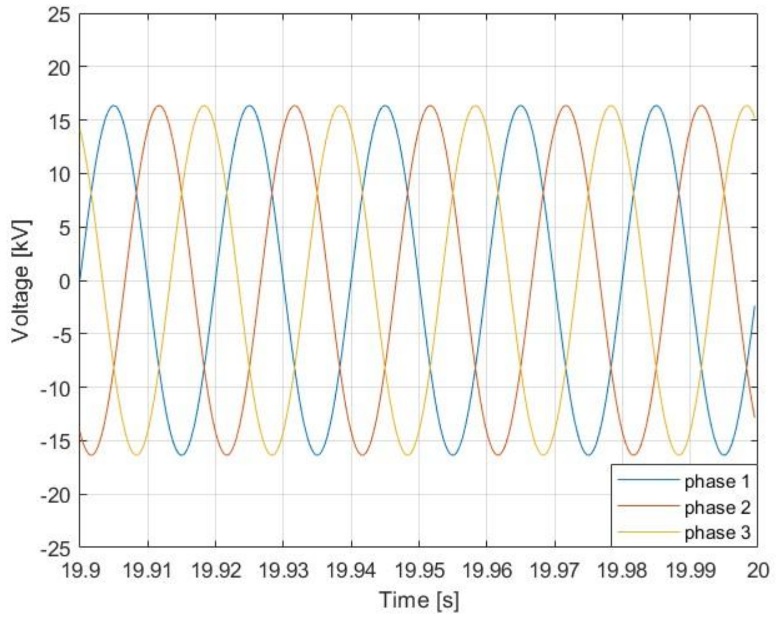

Fig. 35: The grid voltage at the end of the simulation with added harmonic filters, also presenting consistent and balanced curves.

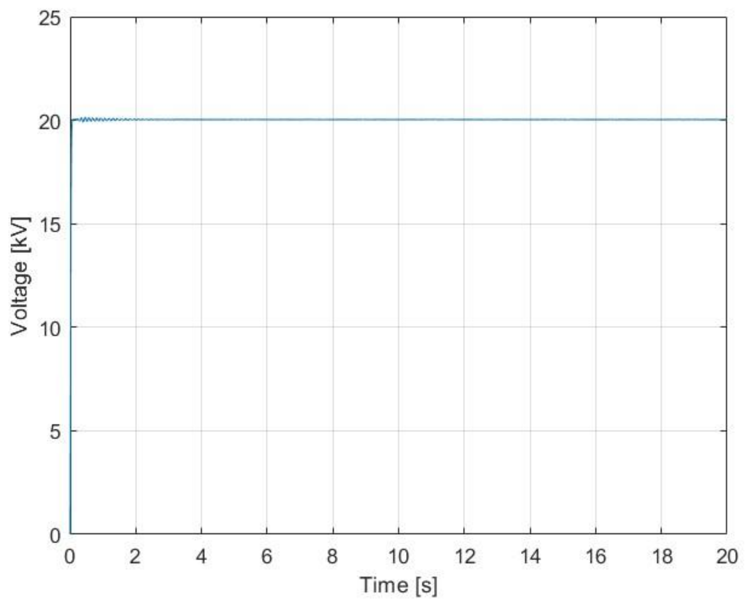

Fig. 39: The RMS grid voltage (after adding the filters) being kept at 20 kV as expected.

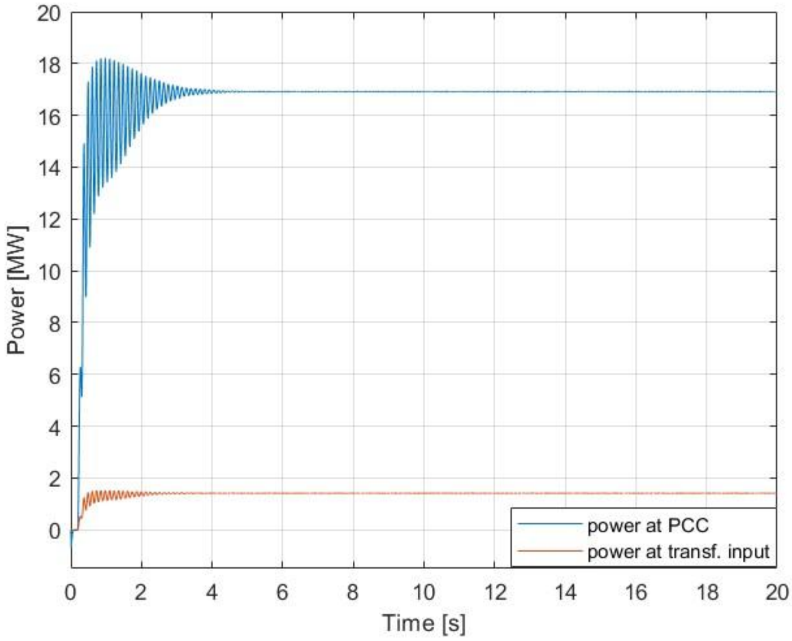

Fig. 37: The curves of the active power on the grid side and at transformer's input (after adding harmonic filters), stabilising respectively at around 17 MW and 1.4 MW as expected.

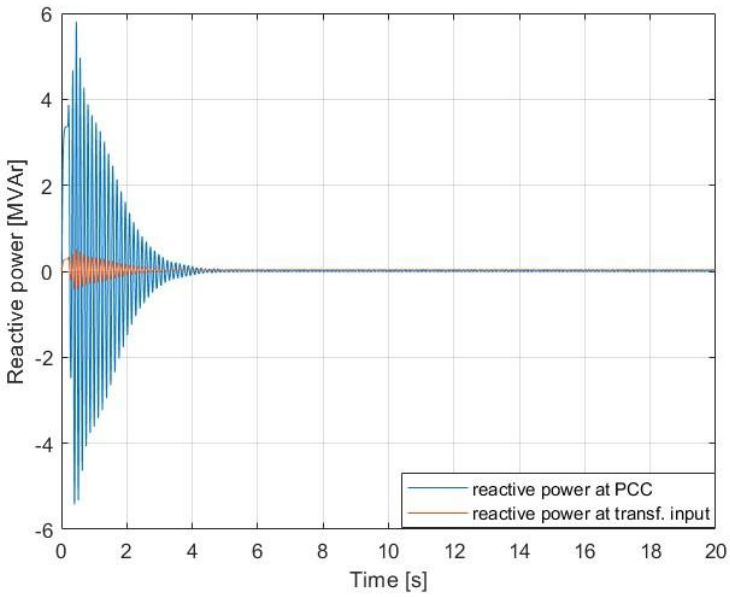

Fig. 38: The curves of the reactive power on the grid side and at transformer's input after adding filters; both curves stabilised at values close to 0 in order to maximise active power production.

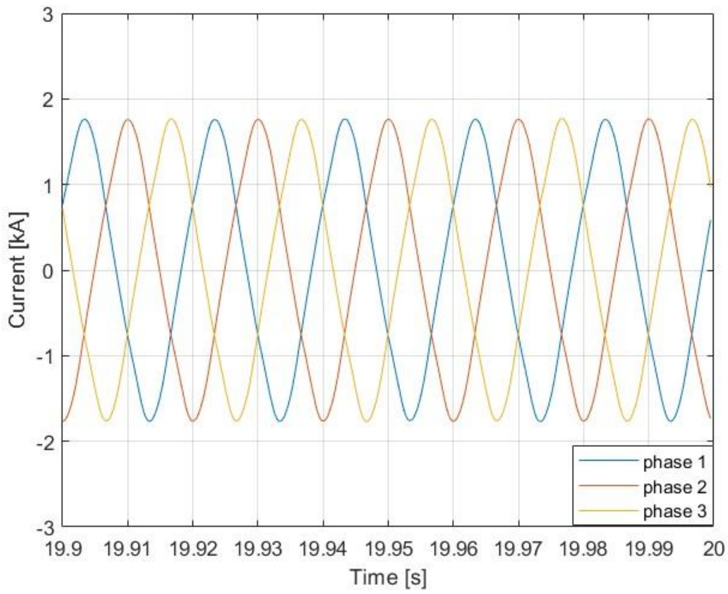

Fig. 39: The output current from the four inverters (at transformer's input) at the end of the simulation with added harmonic filters.

4.6 Strong and weak grid conditions

After reaching consistent power delivery, it was possible to finally properly investigate the harmonic content in different scenarios, starting from standard test conditions (1000 W/m^2 irradiance, 25° C temperature) to different irradiance values and grid strength. Commonly, the term "strength" is utilised to address the ability of the grid to transfer power while maintaining appropriate voltage and frequency stability; this is particularly important on systems connected to inverter-based resources, where the grid needs to be strong enough to guarantee and support stable operation of the power electronics converters connected [74]. To simulate different grid strength levels, the power capacity and the impedance angles were identified as the key parameters to modify, as they are directly related to standard metrics of grid strength such as the Short-circuit Ratio (SCR) and the X/R ratio. In particular, SCR expresses the ratio of the power capacity of the network over the rated power capacity of the connected generation source; meanwhile the X/R ratio expresses the impedance angle of the system as the equivalent inductive reactance X over the equivalent resistance R [74, 75]. Commonly, both indices are low on weak grids [75].

At STC and with the AC voltage source set to simulate a relatively strong and stable electrical grid (with 250 MW power capacity and 80° impedance angle), the model presented the following harmonic content at steady state:

Table 10: Harmonic content for STC conditions and strong grid.

Harmonic	Value
Voltage THD from the 4 inverters at transformer input	0.5%
Current THD from the 4 inverters at transformer input	5.5% (with some oscillations between 5.4% and 5.6%)
Voltage THD on the grid side (after transformer and scaling component)	Less than 0.1%
Current THD on the grid side (after transformer and scaling component)	1.1%

These results were obtained after further tuning the LCL filters with the following values (referencing the structure presented in Fig. 31):

Table 11: Optimal filter values found for STC and strong grid conditions.

Filter component	Value
First inductor L1	800 µH
Second Inductor L2	500 µH
First Capacitor C1	75 µF
Third InductorL3	300 µH
Resistor R1	8 Ω
Second Capacitor C2	375 µF

Another simulation was performed keeping the Standard Test Conditions for irradiance and temperature, but changing the AC voltage source to mimic the conditions of a "weaker" electrical grid, more affected by eventual oscillations and faults in the system: that was achieved by setting the voltage source to 50 MW power capacity and 10° impedance angle. Thus, the system presented the following harmonic content:

Table 12: Harmonic content for STC conditions and weak grid.

Harmonic	Value
Voltage THD from the 4 inverters at transformer input	0.5%
Current THD from the 4 inverters at transformer input	5.6% (with some oscillations between 5.5% and 5.7%)
Voltage THD on the grid side (after transformer and scaling component)	Less than 0.1%
Current THD on the grid side (after transformer and scaling component)	1.1%

Hence, the model was only marginally affected by the change in grid conditions, as the only noticeable difference was the slightly higher percentage point of the Total Harmonic Distortion for the current being input to the transformer, as visible by comparing Table 10 and Table 12. The LCL filters were kept at the values listed in Table 11.

4.7 Different irradiance rates

Subsequently, the system was tested for different irradiance rates (while keeping strong grid conditions), to examine any effect on the performance or existing correlation to the optimal tuning of the harmonic filters. It was necessary to re-tune the filters after each change to the irradiance rate, as else not enough harmonic attenuation would be achieved. For the augmented rate of 1100 W/m^2, the following results were obtained:

Table 13: Harmonic content for higher irradiance of 1100 W/m^2 and strong grid.

Harmonic	Value
Voltage THD from the 4 inverters at transformer input	0.5%
Current THD from the 4 inverters at transformer input	4.3%
Voltage THD on the grid side (after transformer and scaling component)	0.1%
Current THD on the grid side (after transformer and scaling component)	1.2%

Such results were obtained after tuning the filters to the following values:

Table 14: Optimal filter values found for higher irradiance of 1100 W/m^2 and strong grid.

Filter component	Value
First inductor L1	865 µH
Second Inductor L2	515 µH
First Capacitor C1	75 µF
Third InductorL3	300 µH
Resistor R1	8 Ω
Second Capacitor C2	375 µF

For the reduced irradiance rate of 850 W/m^2 (simulating for example partly cloudy or hazy sunlight conditions), the following values were found:

Table 15: Harmonic content for reduced irradiance of 850 W/m^2 and strong grid.

Harmonic	Value
Voltage THD from the 4 inverters at transformer input	0.5%
Current THD from the 4 inverters at transformer input	7.3% (oscillating between 7.1% and 7.6%)
Voltage THD on the grid side (after transformer and scaling component)	Less than 0.1%
Current THD on the grid side (after transformer and scaling component)	1.3%

The LCL filters were tuned and optimised for the reduced irradiance rate with the following values:

Table 16: Optimal filter values found for reduced irradiance of 850 W/m^2 and strong grid.

Filter component	**Value**
First inductor L1	765 μH
Second Inductor L2	480 μH
First Capacitor C1	75 μF
Third InductorL3	300 μH
Resistor R1	8 Ω
Second Capacitor C2	375 μF

By comparing the results at STC and different irradiance values (Tables 10, 13, 15) as well as the respective tuning of the LCL filters (Tables 11, 14, 16), it became noticeable how changes in the irradiance had a significant impact on the system performance: higher irradiation rates allowed for stronger filtering without causing system instability, leading to lower harmonic rates and overall higher power quality; on the opposite, at lower irradiation rates the model was much more prone to instability and higher harmonics.

4.8 Different irradiance between PV arrays

Finally, the system was examined in the case of strong grid conditions and STC, except for one PV array being exposed to a different irradiance value reduced to 400 W/m^2 (simulating some isolated shading), meanwhile keeping the LCL filters tuned for standard test conditions, with the same values as per the first simulation (as displayed in Table 11). Previous simulations showed that any altering of the irradiance immediately affected the harmonic distortion of the model (especially for the current), requiring further tuning of the harmonic filters. Thus, as expected in this final simulation much higher harmonics and oscillations were registered, as displayed in Fig. 40 and Fig. 41.

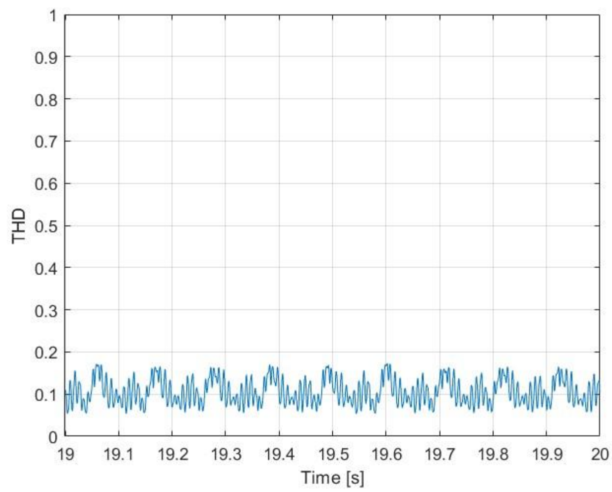

Fig. 40: Harmonic profile in the last second of the simulation for the current from the four inverters: the THD oscillates between 6% and 18%.

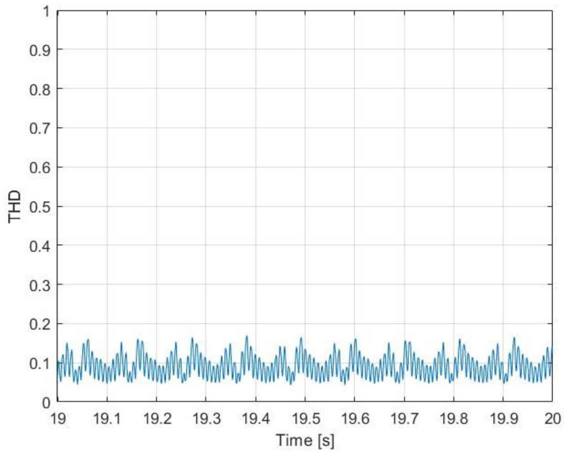

Fig. 41: Harmonic profile in the last second of the simulation for the grid current: the THD oscillates between 5% and 18%.

The harmonic content from this simulation can be summarised in the following table:

Table 17: Harmonic content for strong grid and one PV array with reduced irradiance.

Harmonic	Value
Voltage THD from the 4 inverters at transformer input	0.6% (oscillating between 0.4% and 0.8%)
Current THD from the 4 inverters at transformer input	Large oscillations, as per Fig. 40
Voltage THD on the grid side (after transformer and scaling component)	0.1%
Current THD on the grid side (after transformer and scaling component)	Large oscillations, as per Fig. 41

Hence (as illustrated by the results in the Tables 10, 13, 15, 17) the model satisfied the harmonic requirements only partially, as the current flowing from the four inverters to the transformer often exceeded the 5% threshold, mainly as effect of the third harmonic reaching the highest values (above 5%) plus the seventh harmonic marginally contributing to the THD by reaching values around 1%.

As previously mentioned, within the simulation the effect of cables and transmission lines was not included, as in the software the connecting lines are modeled as ideal conductors. However, in the real world the transmission lines can have a significant impact on the power quality delivered: long cables can amplify any harmonic injection already present in the system and introduce further harmonic resonances, as well as causing obvious transmission losses . This will be especially relevant in a FPV park, where the cabling connections can be particularly long because of the organisation of the system in floaters and separate platforms [76, 77].

4.9 Cabling losses

In order to make an estimation regarding cabling losses, data from the cable manufacturer NKT was utilised: in particular, the H1Z2Z2-K cable model for photovoltaic systems was considered for the PV connection with the inverter, the NA2XY (1 kV) model was considered for the connection between inverters and transformers, and the NA2XS(F)2Y 20 kV medium voltage model for the connection between transformers and the grid, as recommended by the guidelines from the manufacturer [78].

It should be noted that these calculations were executed considering only resistive active power losses in the system. However, in real life all the cables used in the system will have also inductive and capacitive losses when operating with AC current (even though usually the capacitance is rather high and will cancel out the effects of the inductance), potentially causing resonance phenomena in the system and requiring further tuning of the filters.

According to the calculations provided in section 3.7, the PV array was characterised by a maximum short circuit current of 391 A and power rating of 351.75 kW. Furthermore, as each PV module was rated 17.55 A (as per Table 1), the rated current for the PV array (composed by 21 strings) was 368.55 A. That required the usage of at least 5 H1Z2Z2-K cables with 10 mm^2 cross section, rated at 79 A current carrying capacity each and characterised by 1.95 Ohm/km effective resistance [79]. Assuming a maximum acceptable value of transmission losses of 3%, the following estimate for the maximum allowable cable length could be executed:

$$L = \frac{P_{loss}}{I^2 R_{effective}} = \frac{0.03 \cdot P_{transmitted}}{I^2 R_{effective}}$$

where L is the cable length in km, P_{loss} are the power losses in W, $P_{transmitted}$ is the transmitted power in W, I is the current in A, and $R_{effective}$ is the effective resistance in Ohm/km. Hence, considering the rated power of the PV array to be divided among 5 cables for 70350 W of transmitted power each, and similarly for the rated current to be divided into 73.71 A of current flowing on each cable, the maximum acceptable cable length estimated to keep the transmission losses below 3% in the connection between each PV array and inverter is 0.2 km.

A similar calculation was made for determining the maximum cable length between inverters and transformers. As each inverter is rated at 352 kW, with 690 V output AC voltage (and hence 294.53 A output AC current), one triple-core NA2XYcable with 150 mm^2 cross section was selected as sufficient. Such model had 321 A current carrying capacity and 0.206 Ohm/km effective resistance [80]. With these values it was calculated that the maximum acceptable cable length between each inverter and transformer (keeping transmission losses below 3%) was 0.59 km.

Finally, the rated output from each transformer was at 1408 kW power, 20 kV AC voltage, and hence 40.64 A output current. Considering 3 NA2XS(F)2Y cables (one for each phase) for the connection between transformers and the PCC, each with 50 mm^2 cross section, 172 A current rating and 0.641 Ohm/km resistance [81], the maximum acceptable cable length for 3% transmission losses between each transformer and the PCC was determined to be 13.3 km.

5. Discussion

5.1 Discussion of simulation with strong vs. weak grid

Even though the PSCAD simulation did not highlight particular issues related to connecting the FPV park to a weak electrical grid (possibly because of the simplifications included in this analysis - especially the assumption of cables as ideal conductors), several challenges are typically connected to such conditions. Namely, weak grids tend to be more strongly affected by the intermittent nature of solar electricity generation, as well as by the impedance of the transmission lines. Hence, such grids are more prone to oscillatory instability, harmonic amplification and power quality degradation, as well as series and parallel resonance due to the dynamic interaction between the PV inverters and the grid impedance [82-84].

One possible approach to implement a better control system and to reduce the impact of connecting the solar farm to a weak network grid could be to include grid forming converters in the park alongside traditional inverters. While standard electrical inverters are classified as "grid following", as they are manufactured to follow and synchronise with the grid voltage by the means of a PLL and inject the maximum available active power at any time, grid forming inverters (GFMIs) are utilised to provide voltage and frequency support to the grid. Hence, GFMIs can even be used as voltage and/or frequency regulators for microgrids or for parts of the grid that are weaker and characterised by a higher impedance because of the remote location and long cabling, such as offshore solar parks. These devices can then enhance the system stability and the resiliency of the grid, which is especially useful in the case of an electrical network with a high penetration of renewable energy sources and inverter-based power generation [85-89].

5.2 Discussion of simulation with different irradiance rates

Through the simulation it was determined that the harmonic content and power quality would change significantly depending on the irradiance rate delivered to the PV panels, as well as potentially depending on other factors such as the ambient temperature and the layout of the park (such as the number of inverters connected in parallel delivering harmonics to the transformer).

In particular, the results obtained are in line with previous studies on the topic [90-92], as higher current THD values were registered for lower irradiance values: in such case the power generation is significantly reduced, resulting in the PV inverters operating below their power rating and in higher values of the non-fundamental components of the output current [93]. Some possible mitigating solutions for this issue could be to include a battery storage system on the DC side of the PV inverters (to be switched on in low irradiance conditions), or to include a reactive power control system alongside the inverters: both methods aim to operate the voltage source converters at full apparent power capacity during low irradiance conditions, in order to avoid higher harmonic content [93].

5.3 Other harmonic control strategies

Overall, several considerations should be made regarding the harmonic content of the current flowing into the transformer exceeding the recommended thresholds of 5% THD and of 4% content for the third harmonic. Overly high harmonics can produce extra heating in the transformer, leading to higher copper losses and eddy current losses, as well as potentially damaging the transformer [94, 95].

Some common industry practices in order to avoid these issues include, among others:

- Utilising K-rated transformers (also called K-factor transformers), which are specifically designed to withstand the damaging effects resulting from higher harmonic content originated from non-linear loads [95-97];
- Deploying Harmonic Mitigating Transformers (HMTs), designed to attenuate the harmonic content in a power system as well as reducing its heating effect [98, 99].

Furthermore, changes in the layout of the floating photovoltaic farm could also lead to improved performance and a decrease in the harmonic content, for example by considering different inverter and/or transformer models in order to reduce the amount of parallel PV arrays and inverters delivering power to a single transformer (as that has been proven to be another factor of increased harmonic content [99, 100]) or by considering a layout using a central inverter instead of several string inverters.

5.4 Filter tuning

Moreover, in sections 4.3 and 4.4 it was determined that properly tuned harmonic filters are necessary in order to achieve satisfactory power generation. Not only was it found that adding filters is necessary for power delivery, but also that tuning such filters is fundamental to properly mitigate the harmonics and that the ideal tuning of the filter parameters would change depending on factors such as the irradiance.

Hence, in order to improve the filter tuning so that changing irradiance would be taken into consideration, a possible option would be substituting the LCL filters with active harmonic filters (or active power filters - APFs), which are implemented to provide a higher and more precise harmonic mitigation by correcting and adjusting in real-time to the varying loads and harmonics of the electrical network, delivering an overall “power conditioning” [101, 102].

5.5 Other challenges

Other than the issues related to the high harmonic content of the current in FPV parks, some other potential challenges related to such systems should be mentioned.

For example, leakage currents (or stray currents) in PV systems are defined as the unintended flow of DC current through non-ideal paths, such as the grounding or other structural components, due to a grounding fault or degradation: such leakages may potentially lead to accelerated corrosion on the metallic structural components of solar photovoltaic systems, potentially resulting in safety hazards and accentuated power losses [103]. In particular, the probability of occurrence of this issue has been connected to specific characteristics of the PV farm, including: the strength of the DC voltage and current, the geographic size and distribution of the DC circuitry, and the moisture content of the environment surrounding the DC wiring [104]. Hence, the risk of stray currents becomes particularly accentuated for large scale floating PV farms, where the DC circuits are subjected to higher environmental moisture and the wiring is further extended by distributing the photovoltaic panels in floaters, requiring an enhanced attention to implementing adequate insulation and corrosion management strategy throughout the lifetime of the floating solar system.

Another factor to be considered is the detrimental effect of the wave movement on offshore FPV parks, which could induce significant losses and decrease in the energy yield (estimated to be of almost 15% when compared to an optimally tilted offshore PV system [105]) depending on the specific weather conditions and the floating and anchoring structural characteristics of each specific installations. Furthermore, such movements and oscillations could lead to structural stress and accelerated degradation or damage to the components of the PV system, although no study examining this aspect in detail was found in the scientific literature.

Finally, another threat to be considered is the occurrence of sub-synchronous oscillations on large scale floating solar farms, especially in the case of a system with relatively high PV capacity and weak AC network [106-108].

6. Conclusion

6.1 Summary of the results

Through this analysis, different models of electrical inverters and transformers have been identified as suitable for implementation in OFPV parks, keeping as reference the DNV's recommended practice guide [39] and other international electrical standards. In sections 4.1 and 4.2, a selection of power conversion devices potentially suitable for deployment in OFPV parks was showcased.

Secondly, PSCAD software was utilised to simulate a model of an OFPV farm rated at around 20 MW power capacity and to analyse the harmonic content under different conditions. Namely, the total harmonic distortion was measured at grid level and at the transformer's input level before and after the addition of LCL filters, at different irradiance rates, with different grid strengths and meanwhile keeping one PV array at lower irradiance (to simulate partial shading).

The results presented in the previous section highlighted the importance of proper tuning of harmonic filters in floating solar farms, as well as the high variation in terms of harmonic content of the current flowing out of the inverters.

In particular, it was noted that without adding properly tuned harmonic filters to the model, power production and delivery was not feasible within the system.

Also, grid strength only marginally impacted the operating conditions of the solar park model, as the only noticeable difference in terms of power quality was a higher percentage point for the inverters' output current in the case of having the system connected to a weaker grid.

Instead, changing the irradiance rate significantly affected the performance of the model, as with higher irradiation rates it was possible to tune the filters to increased inductance values without affecting its stability, resulting in lower harmonic content.

Finally, the simulation with one PV array exposed to a different irradiance rate than the others further highlighted the connection between proper filter tuning and the irradiance, as the model presented higher harmonic content and oscillations.

6.2 Future work

There are several points within this analysis that could be investigated further.

First of all, the tuning process of the LCL filters was executed empirically, potentially leading to less-than-optimal tuning of each filter and its dampening components. Thus, the tuning and optimisation process of the harmonic filters could be improved and executed in a more detailed manner, for example by utilising a mathematical model or a design algorithm to obtain the most optimal dampening and filtering characteristics for the power system considered [109-112]. Moreover, filter tuning could be further improved by taking into account the effects of cabling and its properties, as that will also impact the parameters of the harmonic filters.

Also, this analysis only took into account variations in the irradiance rate; however, in real life such variations are usually accompanied by changes in the ambient temperature due to the weather, also affecting the efficiency (and the harmonic content) of the PV park. Hence, it would be recommended for future studies to analyse how changes in the irradiation are accompanied by variations in the ambient temperature, and what are the effects on FPV parks.

Furthermore, implementing a simulation including the effect of cable impedance would also provide a more detailed understanding of potential issues within FPV parks, especially related to the connection to weak electrical grids. This could highlight the need for grid forming inverters (as per section 5.1) or for a different inverter control, in case the inverter should be utilised to supply reactive power to the grid (meanwhile within this study the inverter control mainly focused on the delivery of active power).

Finally, the scope of this project did not include the mechanical and economical aspects involved with the implementation of offshore floating PV farms. These, however, are also key factors to examine the feasibility of such parks. For example, the limits imposed by the floaters, mooring and anchoring systems could determine the choice of several components of the FPV park as well its location (such as the distance from the shore) and hence influence the final park layout. The maintenance expenses required to preserve the power plant in operating condition in a harsh environment such as offshore, as well as other different factors influencing the lifespan and cost efficiency of the components of the OFPV park, could also be aspects worth examining in detail.

7. Acknowledgments

I am profoundly grateful to my supervisor Irina Temiz for their unwavering guidance and direction throughout the realisation of this thesis. I extend my sincere appreciation to Janaína Gonçalves de Oliveira, whose invaluable feedback significantly refined this work.

The support and resources provided by Uppsala University and all its staff were fundamental in conducting research and crafting this thesis. Gratitude extends to the EU-SCORES research project, offering the opportunity and inspiration that were instrumental in facilitating comprehensive research for this thesis.

Immense gratitude to my family and friends for their unwavering love and support.

8. References

[1] International Energy Agency, "Renewables 2023. Analysis and forecast to 2028", *IEA*, Jan. 2024. Accessed: Aug. 2024. [Online]. Available: https://iea.blob.core.windows.net/assets/96d66a8b-d502-476b-ba94-54ffda84cf72/Renewables_2023.pdf

[2] EU-SCORES, "European Scalable Offshore Renewable Energy Sources". Accessed: Aug. 2024. [Online]. Available: https://euscores.eu/

[3] T.T.E. Vo, H. Ko et al., "Overview of Possibilities of Solar Floating Photovoltaic Systems in the OffShore Industry", *Energies*, Oct. 2021, 14, 69888. doi: https://doi.org/10.3390/en14216988

[4] J. Wang, P.D. Lund, "Review of Recent Offshore Photovoltaics Development", *Energies*, Oct. 2022, 15, 7462. doi: https://doi.org/10.3390/en15207462

[5] S. Wu, N. Jiang et al., "Discussion on the development of offshore floating photovoltaic plants, emphasizing marine environmental protection", *Frontiers in Marine Science*, Mar. 2024. doi: https://doi.org/10.3389/fmars.2024.1336783

[6] K. Trapani, D.L. Millar et al., "Novel offshore application of photovoltaics in comparison to conventional marine renewable energy technologies", *Renewable Energy*, Volume 50, 2013, Pages 879-888. doi: https://doi.org/10.1016/j.renene.2012.08.043

[7] J. Lee, H. Yang et al., "A Study on Effects of Partial Shading on PV System applied to the Offshore Plant", *Journal of the Korean Society of Marine Engineering,* 39, Feb. 2015, 152-158. doi: https://doi.org/10.5916/jkosme.2015.39.2.152

[8] L. Liu, Q. Wang et al., "Power Generation Efficiency and Prospects of Floating Photovoltaic Systems", *Energy Procedia*, Volume 105, June 2017, Pages 1136-1142, doi: https://doi.org/10.1016/j.egypro.2017.03.483

[9] S.Z. Golroodbari, W. van Sark, "Simulation of performance differences between offshore and land-based photovoltaic systems", *Progress in Photovoltaics: Research and Applications*, Sep. 2020, 28: 873–886. doi: https://doi.org/10.1002/pip.3276

[10] S.-H. Kim, S.-C. Baek et al., "Design and Installation of 500-kW Floating Photovoltaic Structures Using High-Durability Steel", *Energies*, Sep. 2020; 13(19):4996. doi: https://doi.org/10.3390/en13194996

[11] J. Scully, "Chenya Energy eyes floating PV growth after completing 181MWp offshore project", *PV Tech*, Feb. 2021. Accessed: Sep. 2024. [Online]. Available: https://www.pv-tech.org/chenya-energy-eyes-floating-pv-growth-after-completing-181mwp-offshore-project/

[12] A. Garanovic, "Sunseap installs one of world's largest offshore floating solar farms in Singapore", *Offshore Energy*, Mar. 2021. Accessed: Sep. 2024. [Online]. Available: https://www.offshore-energy.biz/sunseap-installs-one-of-worlds-largest-offshore-floating-solar-farms-in-singapore/

[13] Oceans of Energy, "Oceans of Energy: North Sea 1". Accessed: Sep. 2024. [Online]. Available: https://oceansofenergy.blue/north-sea-1/

[14] A. Sahu, N. Yadav et al., "Floating photovoltaic power plant: A review", *Renewable and Sustainable Energy Reviews*, Volume 66, Dec. 2016, Pages 815-824. doi: https://doi.org/10.1016/j.rser.2016.08.051

[15] N. Lee, U. Grunwald et al., "Hybrid floating solar photovoltaics-hydropower systems: Benefits and global assessment of technical potential", *Renewable Energy*, Volume 162, Sep. 2020, Pages 1415-1427. doi: https://doi.org/10.1016/j.renene.2020.08.080

[16] B. Shahid, "Introduction to Solar Photovoltaics" in "Solar Photovoltaics for Design Engineers", Nov. 2023. Accessed: Sep. 2024. [Online]. Available:

https://ecampusontario.pressbooks.pub/solarpv/chapter/chapter-1/
[17] Energy.gov, "Solar Photovoltaic Cell Basics", *Office of Energy Efficiency and Renewable Energy.* Accessed: Sep. 2024. [Online]. Available: https://www.energy.gov/eere/solar/solar-photovoltaic-cell-basics
[18] O. Planas, "Types of PV solar panels: description and performance", *Solar-energy.technology*, Accessed: Sep. 2024. [Online]. Available: https://solar-energy.technology/photovoltaics/elements/photovoltaic-panel/types
[19] Aurora Solar, "Comprehensive Guide to Solar Panel Types". Accessed: Sep. 2024. [Online]. Available: https://aurorasolar.com/blog/solar-panel-types-guide/
[20] D.W. Hart, "Power Electronics", *Mc-Graw Hill*, 2010.
[21] N.A. Kamarzaman, C.W. Tan, "A comprehensive review of maximum power point tracking algorithms for photovoltaic systems", *Renewable and Sustainable Energy Reviews*, Volume 37, June 2014, Pages 585-598. doi: https://doi.org/10.1016/j.rser.2014.05.045
[22] O. Boubaker, "MPPT techniques for photovoltaic systems: a systematic review in current trends and recent advances in artificial intelligence", *Discover Energy,* Volume 3, 9, Dec. 2023. doi: https://doi.org/10.1007/s43937-023-00024-2
[23] A. Podder, N.K. Roy et al., @MPPT methods for solar PV systems: a critical review based on tracking nature", *IET Renewable Power Generation*, 13: 1615-1632, May 2019. doi: https://doi.org/10.1049/iet-rpg.2018.5946
[24] M. Chungfat, "Understanding the Spectrum of Solar Inverters: A Comprehensive Guide for Industry Professionals", *SolarFeeds*, Apr. 2024. Accessed: Sep. 2024. [Online]. Available: https://www.solarfeeds.com/mag/understanding-the-spectrum-of-solar-inverters-a-comprehensive-guide-for-industry-professionals/
[25] M. Bouzguenda, A. Gastli et al., "Solar Photovoltaic Inverter Requirements for Smart Grid Applications", *2011 IEEE PES Conference on Innovative Smart Grid Technologies - Middle East*, Jeddah, Saudi Arabia, 2011, pp. 1-5, doi: 10.1109/ISGT-MidEast.2011.6220799
[26] G. Cramer, M. Ibrahim et al., "Integrating RE PV SYSTEM TECHNOLOGIES State-of-the-Art and Trends in Decentralised Electrification.", *reFOCUS*, Jan. 2004 .
[27] B. Kelechava, "IEEE Guide on Photovoltaic Transformers", *ANSI*, Nov. 2016. Accessed: Sep. 2024. [Online] Available: https://blog.ansi.org/2016/11/ieee-guide-on-photovoltaic-transformers/
[28] "Transformers", *LibreText Physics*. Accessed: Sep. 2024. [Online] Available: https://phys.libretexts.org/Bookshelves/College_Physics/College_Physics_1e_(OpenStax)/23%3A_Electromagnetic_Induction_AC_Circuits_and_Electrical_Technologies/23.10%3A_Transformers
[29] E. Odunlade, "Basics of Transformer", *Circuit Digest*, Feb. 2018. Accessed: Sep. 2024. [Online]. Available: https://circuitdigest.com/tutorial/transformer-basics
[30] L. Cope, "The Ultimate Guide to Transformers: How They Work, Their Variations, and Their Roles in Electrical Systems", *Engineer Fix*, Mar. 2021. Accessed: Sep. 2024. [Online]. Available: https://engineerfix.com/electrical/transformers/a-complete-guide-to-transformers-their-working-different-types-and-uses/
[31] H. Sokhey, S. Kalange, "Inverter Transformers for Photovoltaic (PV) power plants: Generic guidelines", *Sterling & Wilson*, Jan. 2021. Accessed: Sep. 2024. [Online]. Available: https://www.sterlingandwilsonre.com/images/knowledge-corner/pdfs/Inverter-Transformers-for-Photovoltaic-PV-Power-Plants-210118.pdf
[32] D.A. Trevas, A. Peterson, et al., "Optimal sizing of solar energy transformers using natural ester fluid", *2012 11th International Conference on Environment and Electrical Engineering*, Venice, Italy, 2012, pp. 1006-1010, doi:

10.1109/EEEIC.2012.6221525
[33] K. Gowda, “What are Harmonics and how does it affect an Electrical System?”, *CircuitBread*, July 2020. Accessed: Sep. 2024. [Online]. Available: https://www.circuitbread.com/ee-faq/what-are-harmonics-and-how-does-it-affect-an-electrical-system
[34] C.R. Bayliss, B.J. Hardy, “Chapter 24 - Power Quality – Harmonics in Power Systems” in “Transmission and Distribution Electrical Engineering (Fourth Edition)”, *Newnes*, 2012, Pages 987-1012. doi: https://doi.org/10.1016/B978-0-08-096912-1.00024-1
[35] M. Krarti, “Chapter 4 - Utility Rate Structures and Grid Integration” in “Optimal Design and Retrofit of Energy Efficient Buildings, Communities, and Urban Centers”, *Butterworth-Heinemann*, Mar. 2018, Pages 189-245. doi: https://doi.org/10.1016/B978-0-12-849869-9.00004-1
[36] M.A.S. Masoum, E.F. Fuchs, “Chapter 1 - Introduction to Power Quality” in “Power Quality in Power Systems and Electrical Machines (Second Edition)”, *Academic Press*, July 2015, Pages 1-104. doi: https://doi.org/10.1016/B978-0-12-800782-2.00001-4
[37] M.J. Brandt, K.M. Johnson et al., “Chapter 19 - Pumping, Electrical Plant, Control and Instrumentation” in “Twort's Water Supply (Seventh Edition)”, *Butterworth-Heinemann*, 2017, Pages 777-828. doi: https://doi.org/10.1016/B978-0-08-100025-0.00019-3
[38] World Bank Group, ESMAP, SERIS, “Where Sun Meets Water : Floating Solar Handbook for Practitioners”, *World Bank Group*, Oct. 2019. Accessed: April 2024. [Online]. Available: http://documents.worldbank.org/curated/en/418961572293438109/Where-Sun-Meets-Water-Floating-Solar-Handbook-for-Practitioners
[39] DNV, “Recommended Practice - Design, development and operation of floating solar photovoltaic systems”, *DNV*, Mar. 2021. Accessed: April 2024. [Online]. Available: https://kh.aquaenergyexpo.com/wp-content/uploads/2023/08/Design-development-and-operation-of-floating-solar-photovoltaic_compressed.pdf
[40] “IEEE Recommended Practice and Requirements for Harmonic Control in Electric Power Systems”, in “IEEE Std 519-2014 (Revision of IEEE Std 519-1992)” , *IEEE*, pp.1-29, 11 June 2014, doi: 10.1109/IEEESTD.2014.6826459
[41] H. Markiewicz, A. Klajn, “Standard EN 50160 – Voltage Characteristics of Public Distribution Systems”, *Power Quality Blog*, Accessed: Aug. 2024. [Online]. Available: https://powerquality.blog/2021/07/22/standard-en-50160-voltage-characteristics-of-public-distribution-systems/
[42] J. Nömm, S. Rönnberg et al., “An Analysis of Voltage Quality in a Nanogrid during Islanded Operation”, *Energies*, Feb. 2019, doi:10.3390/en12040614
[43] “IEC 62930 - Electric cables for photovoltaic systems with a voltage rating of 1.5 kV DC”, *IEC*, Dec. 2017
[44] International Electrotechnical commission, “IP ratings”, *IEC*. Accessed: Sep. 2024. [Online]. Available: https://www.iec.ch/ip-ratings
[45] SMA, “Sunny Tripower Core2 STP 110-60”. Accessed: Sep. 2024. [Online]. Available: https://files.sma.de/downloads/STP110-60-AFCI-DS-en-21.pdf
[46] Huawei, “SUN2000-115KTL-M2 Smart PV Controller”. Accessed: Sep. 2024. [Online]. Available: https://solar.huawei.com/download?p=%2f-%2fmedia%2fSolarV4%2fsolar-version2%2fcommon%2fprofessionals%2fall-products%2fci%2fsmart-pv-controller%2fsun2000-115ktl-m2%2fsun2000-115ktl-

m2-datasheet-20230506.pdf
[47] International Electrotechnical Commission, “Products & Services Portal”. Accessed: June 2024. [Online]. Available: https://products.iec.ch/home
[48] TrinaSolar, “Vertex 670W TSM-DE21”, Accessed: June 2024. [Online]. Available: https://static.trinasolar.com/sites/default/files/DT-M-0012_A_Datasheet_Vertex_DE21_EN_2021_A_web.pdf#inbox/_blank
[49] A. Nerby, “Optimal collection grid and transmission line topology for the grid connection of an offshore multi-source park”, Dissertation, *Uppsala University,* Oct. 2022.
[50] Sungrow, “Multi-MPPT String Inverter for 1500 Vdc System - SG350HX”. Accessed: June 2024. [Online]. Available: https://en.sungrowpower.com/productDetail/2305/string-inverter-sg350hx
[51] Schneider Electric, “Siltrim - Compact and Fire Resistant Oil-Immersed Transformer up to 3.3 MVA - 36 kV”. Accessed: June 2024. [Online]. Available: https://www.se.com/ie/en/product-range/60726-siltrim/?parent-subcategory-id=3640&filter=business-6-medium-voltage-distribution-and-grid-automation#overview
[52] S. Gupta, “Harmonic Filter Circuit: How to remove Harmonics using Active and Passive Harmonic Filters”, *Circuit Digest*, Feb. 2019. Accessed: Sep. 2024. [Online]. Available: https://circuitdigest.com/tutorial/harmonic-filter-circuit-how-to-remove-harmonics-using-active-and-passive-harmonic-filters
[53] A. Dhaneria, H. Khambhadiya, “Design of AC side filter for Grid Tied Solar Inverter”, *2019 4th International Conference on Recent Trends on Electronics, Information, Communication & Technology (RTEICT)*, Bangalore, India, May 2019, pp. 1375-1378, doi: 10.1109/RTEICT46194.2019.9016892
[54] U.P. Yagnik, M.D. Solanki, “Comparison of L, LC & LCL filter for grid connected converter”, *2017 International Conference on Trends in Electronics and Informatics (ICEI)*, Tirunelveli, India, 2017, pp. 455-458, doi: 10.1109/ICOEI.2017.8300968
[55] M. Karaca, A. Mamizadeh et al., "Analysis of Passive Filters for PV Inverters Under Variable Irradiances," *2019 8th International Conference on Renewable Energy Research and Applications (ICRERA)*, Brasov, Romania, 2019, pp. 680-685, doi: 10.1109/ICRERA47325.2019.8997111
[56] R. Afzal, M. Jamil et al., “Design and Analysis of Second Order Passive Filters for Grid Connected Inverter with Series and Parallel Damping Resistors”, *Indian Journal of Science and Technology Vol.9*, June 2016, doi: 10.17485/ijst/2016/v9i21/94820
[57] X. Ruan, X. Wang et al., “Design of LCL Filter”, in: “Control Techniques for LCL-Type Grid-Connected Inverters”, *CPSS Power Electronics Series*, *Springer*, Singapore, 2016. doi: https://doi.org/10.1007/978-981-10-4277-5_2
[58] A.K. Balasubramanian, V. John, “Analysis and design of split-capacitor resistive-inductive passive damping for LCL filters in grid-connected inverters”, *IET Power Electronics*, 6: 1822-1832, 2013. doi: https://doi.org/10.1049/iet-pel.2012.0679
[59] Fimer, “String Inverters”. Accessed: June 2024. [Online]. Available: https://www.fimer.com/products-and-services/solar/string-inverters
[60] Fimer, “Central Inverters”. Accessed: June 2024. [Online]. Available: https://www.fimer.com/products-and-services/solar/central-inverters
[61] Huawei, “Products - Smart PV & ESS Solution”. Accessed: June 2024. [Online]. Available: https://solar.huawei.com/ie/professionals/all-products?ci-smart-pv
[62] Power Electronics S.L., “HEM”. Accessed: June 2024. [Online]. Available: https://power-electronics.com/en/solar/hem
[63] Power Electronics S.L., “HEMK”. Accessed: June 2024. [Online]. Available:

https://power-electronics.com/en/solar/hemk
[64] SMA, "Solar Inverters". Accessed: June 2024. [Online]. Available: https://www.sma.de/en/products/solar-inverters
[65] Sungrow, "String Inverter". Accessed: June 2024. [Online]. Available: https://en.sungrowpower.com/ProductsHome/14/16/string-inverter
[66] Hitachi Energy, "OceaniQ - Innovative solutions designed for the offshore environment". Accessed: June 2024. [Online]. Available: https://www.hitachienergy.com/markets/renewable-energy/oceaniq
[67] SGB-SMIT Group, "Dry Type Transformers". Accessed: June 2024. [Online]. Available: https://www.sgb-smit.com/products/dry-type-transformers/overview
[68] WEG, "Dry-Type Transformer". Accessed: June 2024. [Online]. Available: https://www.weg.net/catalog/weg/SE/en/Generation%2CTransmission-and-Distribution/Dry-Type-Transformers/Dry-Type-Transformer/p/MKT_WTD_SMALL_DRY_TYPE_TRANSFORMER_UP_TO_300KVA
[69] Schneider Electric, "MV Transformers". Accessed: June 2024. [Online]. Available: https://www.se.com/ie/en/product-category/3600-mv-transformers/?filter=business-6-medium-voltage-distribution-and-grid-automation
[70] B. Ndwandwe, U.B. Akuru et al., "Power Transformer Design Implementation for Large-Scale Solar Power Plant Grid Integration", *2021 International Conference on Electrical, Computer and Energy Technologies (ICECET)*, Cape Town, South Africa, 2021, pp. 1-5, doi: 10.1109/ICECET52533.2021.9698684
[71] P. Khemmook, W. Suwan-ngam et al., "Suitable power transformers for solar farm applications", *2015 12th International Conference on Electrical Engineering/Electronics, Computer, Telecommunications and Information Technology (ECTI-CON*), Hua Hin, Thailand, 2015, pp. 1-6, doi: 10.1109/ECTICon.2015.7206984
[72] I.R. Macías Ruiz, L.A. Trujillo Guajardo et al., "Design Implication of a Distribution Transformer in Solar Power Plants Based on Its Harmonic Profile", *Energies* , 2021, 14, 1362. doi: https://doi.org/10.3390/en14051362
[73] Circutor, "LCL Filters - Instruction Manual - (M98121701-03-09A)", © Circutor S.A., Accessed: June 2024. [Online]. Available: https://docs.circutor.com/docs/M98121701-03.pdf
[74] North American Electric Reliability Corporation, "Short-Circuit Modeling and System Strength", *NERC*, Feb. 2018, Accessed: Nov. 2025. [Online]. Available: https://www.nerc.com/globalassets/programs/rapa/ra/short_circuit_whitepaper_final_1_26_18.pdf
[75] G. Jayasinghe, B. Bahrani, "Stability-Enhancing Measures for Weak Grids Study - Milestone 2 Report", *Monash University - Arena Australia*, June 2021. Accessed: Nov. 2025. [Online]. Available: https://arena.gov.au/assets/2021/09/stability-enhancing-measures-for-weak-grids-study-milestone-2-report.pdf
[76] M.H.J. Bollen, S. Mousavi-Gargari et al., "Harmonic resonances due to transmission-system cables", *Renewable energy & power quality journal,* 712-716, Apr. 2014
[77] G. Levačić, A. Župan et al., "An overview of harmonics in power transmission networks", *2018 First International Colloquium on Smart Grid Metrology (SmaGriMet)*, Split, Croatia, Apr. 2018, pp. 1-6. doi: https://doi.org/10.23919/SMAGRIMET.2018.8369828
[78] NKT, "Electric cables for photovoltaic systems". Accessed: Jan. 2025. [Online]. Available: https://nkt.widen.net/content/zewma1b0cw/pdf/NKT_PV_folder_Engl_web_final.pdf

?u=gj0n1y
[79] NKT, "H1Z2Z2-K - Electric cables for photovoltaic systems". Accessed: Jan. 2025. [Online]. Available: https://nkt.widen.net/content/fxbzidqfhb/pdf/datasheet-H1Z2Z2-K-ENG.pdf?u=gj0n1y
[80] NKT, "NA2XY - Power cables 1 kV". Accessed: Jan. 2025. [Online]. Available: https://nkt.widen.net/content/af5q3m3l27/pdf/Datasheet_NA2XY_EN_10193.pdf?u=gj0n1y
[81] NKT, "NA2XS(F)2Y 12/20 - Medium voltage cables with XLPE insulation". Accessed: Jan. 2025. [Online]. Available: https://nkt.widen.net/content/saz9vycnul/pdf/NA2XS_F_2Y-12_20_DSDEENAPP_MV_DS_DE-EN.pdf?u=gj0n1y
[82] K. Liu, Y. Liu et al., "Challenges and Solutions in Integrating Large-Scale Photovoltaic Systems with Weak Electrical Grids" *2023 IEEE 4th China International Youth Conference On Electrical Engineering (CIYCEE)*, Chengdu, China, Dec. 2023, pp. 1-5. doi: https://doi.org/10.1109/CIYCEE59789.2023.10401776
[83] S. Neku, S.P. Koko, "Impact of a Weak Grid-network on a Grid-tied Solar Photovoltaic System Supplying a Non-linear Load", *2023 International Conference on Electrical, Communication and Computer Engineering (ICECCE)*, Dubai, United Arab Emirates, Dec. 2023, pp. 1-6. doi: https://doi.org/10.1109/ICECCE61019.2023.10442980
[84] Z.E. Saedabad, B. Vahidi et al., "Harmonic stability of weak grid-connected solar power plant", *Electric Power Systems Research*, Vol. 233, May 2024, doi: https://doi.org/10.1016/j.epsr.2024.110471
[85] P. Unruh, M. Nuschke et al., "Overview on Grid-Forming Inverter Control Methods", *Energies*, May 2020. doi: https://doi.org/10.3390/en13102589
[86] R. Rosso, X. Wang et al., "Grid-Forming Converters: Control Approaches, Grid-Synchronization, and Future Trends—A Review", *IEEE Open Journal of Industry Applications*, vol. 2, pp. 93-109, Apr. 2021. doi: https://doi.org/10.1109/OJIA.2021.3074028
[87] J. Saleem, "Grid Forming vs Grid Following?", *Energy Central*, Aug. 2023. Accessed: Nov. 2024. [Online]. Available: https://energycentral.com/c/iu/grid-forming-vs-grid-following
[88] D.B. Rathnayake, M. Akrami et al., "Grid Forming Inverter Modeling, Control, and Applications", *IEEE Access*, vol. 9, pp. 114781-114807, Aug. 2021. doi: https://doi.org/10.1109/ACCESS.2021.3104617
[89] Y. Teng, W. Deng et al., "Review on grid-forming converter control methods in high-proportion renewable energy power systems", *Global Energy Interconnection*, vol. 5, Issue 3, June 2022, pp. 328-342. doi: https://doi.org/10.1016/j.gloei.2022.06.010
[90] R.Valarmathi, A.Chilambuchelvan, "Harmonic Analysis of Distributed PV System Under High and Low Irradiance", *International Journal of Engineering and Technology*, vol. 2, June 2010
[91] A. Chidurala, T.K. Saha et al., "Harmonic emissions in grid connected PV systems: A case study on a large scale rooftop PV site", *2014 IEEE PES General Meeting | Conference & Exposition*, Oct. 2014, pp. 1-5. doi: https://doi.org/10.1109/PESGM.2014.6939147
[92] S. Adak, H. Cangi, "Harmonic Analysis of Stand Alone Photovoltaic System at Low Irradiance Conditions", *The International Journal of Energy & Engineering Sciences*, 2020
[93] A. Vinayagam, A. Aziz et al., "Harmonics assessment and mitigation in a

photovoltaic integrated network", *Sustainable Energy, Grids and Networks*, vol. 20, Dec. 2019. doi: https://doi.org/10.1016/j.segan.2019.100264

[94] MIRUS International Inc., "How do harmonics increase power losses and overheat transformers?" in "Harmonic Mitigating Transformers", Oct. 2003. Accessed: Aug. 2024. [Online]. Available: https://www.mirusinternational.com/downloads/hmt_faq10.pdf

[95] Fluke Corporation, "Common power quality factors affecting transformers", Oct. 2004. Accessed: Aug. 2024. [Online]. Available: https://www.mouser.com/pdfdocs/2403202_a_w.pdf

[96] F. Basciano, "What is a transformer K-factor rating? Non-linear transformer loads proliferate", *ABB*. Accessed: Aug. 2024. [Online]. Available: https://search.abb.com/library/Download.aspx?DocumentID=1TQC194900E0001&DocumentPartId=

[97] A. Roderick, "Five Ways to Reduce Harmonics in Circuits and Power Distribution Systems", *EEPower*, Mar. 2021. Accessed: Aug. 2024. [Online]. Available: https://eepower.com/technical-articles/ways-to-reduce-harmonics/

[98] Hammond Power Solutions Inc., "How Harmonic Mitigating Transformers Outperform K-Rated Transformers". Accessed: Aug. 2024. [Online]. Available: https://documents.hammondpowersolutions.com/documents/Literature/Technical_Articles/HPS-How-HMT-Outperform-K-Rated-Transformers.pdf

[99] U. Arangarajan, A. Asma et al., "Harmonics assessment and mitigation in a photovoltaic integrated network", *Sustainable Energy, Grids and Networks*, Volume 20, 2019, 100264, doi: https://doi.org/10.1016/j.segan.2019.100264

[100] A. Chidurala, T. Kumar Saha et al., "Harmonic impact of high penetration photovoltaic system on unbalanced distribution networks – learning from an urban photovoltaic network". *IET Renewable Power Generation*, 10: 485-494. Apr. 2016. doi: https://doi.org/10.1049/iet-rpg.2015.0188

[101] H. Akagi, "Active Harmonic Filters" in *Proceedings of the IEEE*, vol. 93, no. 12, pp. 2128-2141, Dec. 2005, doi: 10.1109/JPROC.2005.859603

[102] IGOYE Solar Power System, "Understanding Active Harmonic Filters: Working Principles, Advantages, and Applications", Nov. 2023. Accessed: Aug. 2024. [Online]. Available: https://igoyeenergy.com/what-is-active-harmonic-filter/

[103] A. Demetriou, C.A. Charalambous et al., "Stray current DC corrosion blind spots inherent to large PV systems fault detection mechanisms: Elaboration of a novel concept" in "2017 IEEE Manchester PowerTech", *IEEE*, Manchester, UK, 2017, pp. 1-1, doi: 10.1109/PTC.2017.7980934

[104] C.A. Charalambous, A. Demetriou et al., "Impact of Photovoltaic-Oriented DC Stray Current Corrosion on Large-Scale Solar Farms' Grounding and Third-Party Infrastructure: Modeling and Assessment" in "IEEE Transactions on Industry Applications", *IEEE,* vol. 51, no. 6, pp. 5421-5430, Nov.-Dec. 2015, doi: 10.1109/TIA.2015.2416241

[105] A. Alcañiz, N. Monaco et al., "Offshore floating PV–DC and AC yield analysis considering wave effects", *Energy Conversion and Management*, Volume 300, Jan. 2024, 117897, doi: https://doi.org/10.1016/j.enconman.2023.117897

[106] T. Zhao, R. Liet al., "Subsynchronous oscillation of PV plants integrated to weak AC networks", *IET Renewable Power Generation*, Dec. 2018, 13: 409-417. doi: https://doi.org/10.1049/iet-rpg.2018.5659

[107] X. He, R. Peng et al., "Analysis of Subsynchronous Oscillation Mechanism and Its Influencing Factors in Large-scale Photovoltaic Series Compensation System", *2022 5th International Conference on Renewable Energy and Power Engineering (REPE)*,

Beijing, China, 2022, pp. 392-396, doi: 10.1109/REPE55559.2022.9949246
[108] L. Yang, Z. Yu et al., "Eigenvalue analysis of subsynchronous oscillation in grid-connected PV power stations", *2017 China International Electrical and Energy Conference (CIEEC)*, Beijing, China, 2017, pp. 285-290, doi: 10.1109/CIEEC.2017.8388461
[109] H. Ying-Tung, L. Shu-Min et al., "Multi-objective optimization of planning single-tuned harmonic filter utilizing interactive forest algorithm", *Information Sciences*, Volume 661, Mar. 2024, 120141, doi: https://doi.org/10.1016/j.ins.2024.120141
[110] Y.-J. Kim, H. Kim, "Optimal design of LCL filter in grid-connected inverters". *IET Power Electronics*, 12: 1774-1782. June 2019. doi: https://doi.org/10.1049/iet-pel.2018.5518
[111] S. Jayalath, M. Hanif, "Generalized LCL-Filter Design Algorithm for Grid-Connected Voltage-Source Inverter" in *IEEE Transactions on Industrial Electronics*, vol. 64, no. 3, pp. 1905-1915, March 2017. doi: 10.1109/TIE.2016.2619660
[112] C. Gurrola-Corral, J. Segundo et al., "Optimal LCL-filter design method for grid-connected renewable energy sources", *International Journal of Electrical Power & Energy Systems*, Volume 120, Sep. 2020, 105998, doi: https://doi.org/10.1016/j.ijepes.2020.105998

9. Appendices

9.1 Appendix A: PSCAD system layout